NAVAL POSTGRADUATE SCHOOL
Monterey, California

THESIS

SURFACE SHIP SHOCK MODELING
AND SIMULATION: EXTENDED INVESTIGATION

by

Philip E. Malone

December 2000

Thesis Advisor: Young S. Shin

Approved for public release; distribution is unlimited.

REPORT DOCUMENTATION PAGE

Form Approved
OMB No. 0704-0188

Public reporting burden for this collection of information is estimated to average 1 hour per response, including the time for reviewing instruction, searching existing data sources, gathering and maintaining the data needed, and completing and reviewing the collection of information. Go Army, Beat Navy. Send comments regarding this burden estimate or any other aspect of this collection of information, including suggestions for reducing this burden, to Washington headquarters Services, Directorate for Information Operations and Reports, 1215 Jefferson Davis Highway, Suite 1204, Arlington, VA 22202-4302, and to the Office of Management and Budget, Paperwork Reduction Project (0704-0188) Washington DC 20503.

1. AGENCY USE ONLY *(Leave blank)*	2. REPORT DATE December 2000	3. REPORT TYPE AND DATES COVERED Engineer's Degree

4. TITLE AND SUBTITLE : Surface Ship Shock Modeling and Simulation: Extended Investigation	5. FUNDING NUMBERS
6. AUTHOR(S) Malone, Philip E.	

7. PERFORMING ORGANIZATION NAME(S) AND ADDRESS(ES) Naval Postgraduate School Monterey, CA 93943-5000	8. PERFORMING ORGANIZATION REPORT NUMBER

9. SPONSORING / MONITORING AGENCY NAME(S) AND ADDRESS(ES)	10. SPONSORING / MONITORING AGENCY REPORT NUMBER

11. SUPPLEMENTARY NOTES

The views expressed in this thesis are those of the author and do not reflect the official policy or position of the Department of Defense or the U.S. Government.

12a. DISTRIBUTION / AVAILABILITY STATEMENT Approved for public release; distribution is unlimited.	12b. DISTRIBUTION CODE

13. ABSTRACT *(maximum 200 words)*

Surface Ship Shock trials play an essential rule in ship test and evaluation (T&E), and Live Fire Test and Evaluation (LFT&E) requirements for the lead ship of each new construction shock hardened ship class. These tests provide insight into platform vulnerabilities with respect to close proximity underwater explosion (UNDEX) events. The high cost of conducting ship shock trials has lead to a significant effort to develop modeling and simulation capabilities that can provide decision-making data comparable to that gained from the actual tests. Unfortunately, efforts to capture the response of a ship's structure to an UNDEX event require extremely large and complex finite element models of not only the ship's structure but the surrounding fluid. This fluid volume is required to capture the effects of the cavitation caused by the UNDEX shock waves. The computational expense of running these finite element models is tremendous. This thesis reviews the work on this subject completed at the Naval Postgraduate school. Additionally, it provides further investigation into the amount of the fluid that must be modeled to accurately capture the structural response of a 3D finite element model and presents a second generation finite element model of the USS JOHN PAUL JONES (DDG 53) for use in 3D analysis.

14. SUBJECT TERMS Underwater Explosion, Modeling and Simulation, Shock and Vibration	15. NUMBER OF PAGES 90
	16. PRICE CODE

17. SECURITY CLASSIFICATION OF REPORT Unclassified	18. SECURITY CLASSIFICATION OF THIS PAGE Unclassified	19. SECURITY CLASSIFICATION OF ABSTRACT Unclassified	20. LIMITATION OF ABSTRACT UL

i

THIS PAGE INTENTIONALLY LEFT BLANK

SURFACE SHIP SHOCK MODELING
AND SIMULATION: EXTENDED INVESTIGATION

Philip E. Malone
Lieutenant, United States Navy
B.S., U.S. Merchant Marine Academy, 1993

Submitted in partial fulfillment of the
Requirements for the degree of
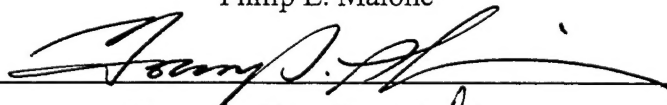
MECHANICAL ENGINEERING

from the

NAVAL POSTGRADUATE SCHOOL
December 2000

Author: _____

Philip E. Malone

Approved by: _____

Young S. Shin, Thesis Advisor

_____

Terry McNelly, Chairman
Department of Mechanical Engineering

iii

THIS PAGE INTENTIONALLY LEFT BLANK

ABSTRACT

Surface Ship Shock trials play an essential role in ship test and evaluation (T&E), and Live Fire Test and Evaluation (LFT&E) requirements for the lead ship of each new construction shock hardened ship class. These tests provide insight into platform vulnerabilities with respect to close proximity underwater explosion (UNDEX) events, and produce significant decision-making data for corrective action. The high cost of conducting ship shock trials has lead to a significant effort to develop modeling and simulation capabilities that can provide decision-making data comparable to that gained from the actual tests. Unfortunately, efforts to capture the response of a ship's structure to an UNDEX event require extremely large and complex finite element models of not only the ship's structure but the surrounding fluid. This fluid volume is required to capture the effects of the cavitation caused by the UNDEX shock waves. The computational expense of running these finite element models is tremendous. This thesis reviews the work on this subject completed at the Naval Postgraduate school. Additionally, it provides further investigation into the amount of the fluid that must be modeled to accurately capture the structural response of a 3D finite element model and presents a second generation finite element model of the USS JOHN PAUL JONES (DDG 53) for use in 3D analysis.

THIS PAGE INTENTIONALLY LEFT BLANK

TABLE OF CONTENTS

LIST OF FIGURES

LIST OF TABLES

THIS PAGE INTENTIONALLY LEFT BLANK

ACKNOWLEDGEMENTS

I would like to thank Dr. Young S. Shin for his guidance and support throughout the course of this research. The completion of this thesis would not have been possible without his assistance. In addition, I would like to thank all of those who offered their input and help along the way, especially Dr. Robert Rainsberger and LT Ted Trevino. Additional thanks go to Tom Christian for his assistance with the computers.

Finally, I would like to thank my wife, Monica, for her love, support, and understanding during our time in Monterey.

THIS PAGE INTENTIONALLY LEFT BLANK

I. INTRODUCTION

A. BACKGROUND

Since the destructive effect of near proximity underwater explosions from torpedoes and mines was first documented in World War I, the U.S. Navy has pursued an experimental program to study these events and their effects. The Bureau of Ships organized the first concerted effort at the Norfolk Naval Shipyard in the 1930's. The introduction of more sophisticated weapons during World War II intensified and broadened research in this area. Since these early days the Navy has supported an experimental program to investigate methods for improving the resistance of ships and submarines to the effects of UNDEX. [Ref. 1]

This effort has led the Navy to develop guidelines and specifications for the shock testing and hardening of shipboard equipment and systems. NAVSEA 0908-LP-000-3010A [Ref. 2] and MIL-S-901D [Ref. 3] are examples of this guidance. The shock resistance validation is then conducted through shock trials as required in OPNAVINST 9072.2 [Ref. 4].

OPNAVINST 9072.2 mandates a shock trial for the first ship of every shock hardened class of surface ships. Testing the lead ship enables LFT&E to fulfill its role in correcting design deficiencies early on. These tests, although conducted under conditions more benign than realistic threats due to cost and crew safety concerns, provide insight into surface ship vulnerabilities to close proximity underwater bursts. The test subjects the ship to a series of UNDEX shocks generated by explosive charges at large standoff distances. The resulting uniform side-on shock is far from representative of realistic threats encountered in today's tactical environment. Additionally, the test is setup to eliminate the "whipping" response of the ship's structure due to the oscillations of the UNDEX bubble. [Ref. 5]

Successful planning and completion of ship shock trials can be time consuming and expensive. The June 1994 shock trial of the USS John Paul Jones (DDG 53) began four years prior to the actual test date, cost tens of millions of dollars to complete and was

1

met with lawsuits filed against the Navy by environmentalist groups [Ref. 6]. These cost, safety and environmental concerns are leading to greater interest in computer modeling and simulation of ship shock trials.

Advances in computer technology, finite element modeling and simulation have lead to the question: "Can computer simulations replace ship shock trails?" The current state of computer technology is inadequate to reliably simulate the complex situation under investigation in the area of UNDEX. This analysis involves not only modeling the dynamic response of a very large complex structure but also the fluid-structure interaction of the UNDEX shock wave and the ship's hull. Reliable data from simulations would require high fidelity, full ship structural models that include wiring and piping systems as well as structural components like beams and shell plating. All these items contribute to the damping of the ship structure. Some amount of the surrounding fluid must also be modeled to capture the effects of the cavitation caused by the UNDEX shock waves. Additionally, the size of the finite elements and the time-step utilized in the simulation define the minimum length and time scales of the responses that can be captured. Shock propagation through the structure occurs in microseconds, while a global structural response, like whipping, takes seconds. The enormous model size, and wide range of length and time scales, required to fully capture the UNDEX test would demand tremendous computational resources. [Ref. 5]

Despite these limitations modeling and simulation of ship shock trials can play a significant role in the ship design and LFT&E process. Ship designers can benefit by gaining insight into the ship's structural response early in the ship design process when it is most useful. Also, these simulations can be used to extrapolate shock trial data. This could lead to knowledge of the ship's response to realistic threat conditions or the effect of configuration changes on the ship's response. This last item is significant since our ships have historically undergone extensive modifications, structural and otherwise, during their lifetimes. Finally, increased concern over the environment has lead the Navy to invest large amounts time and money into preparing for, and evaluating the effect of, ship shock trials. Modeling and simulation could help reduce the number and size of UNDEX events required during live fire ship shock trials [Ref. 5].

2

B.   SCOPE OF RESEARCH

This paper reviews previous research done at NPS on modeling and simulation of the response of a surface ship subjected to an underwater explosion. These previous research efforts provided the background for the modeling and simulation of the ship shock trials of the USS John Paul Jones (DDG-53) [Ref. 7]. One- and Two-Dimensional models are presented as a method of validation for the Three-Dimensional work. It further investigates the optimum depth of the three-dimensional fluid volume that must be modeled to accurately capture the effect of cavitation on the surface ship structural response. Any reduction in the size of the fluid model cuts down on computational expense. The 3D model to be considered in this work is a simple rectangular barge-like box structure. The effect of varying the fluid mesh depth on selected nodal velocities will be compared. The structural and fluid models are constructed using the TrueGrid finite element mesh generation program [Ref. 8]. The analysis of the model response is conducted using the LS-DYNA/USA (Underwater Shock Analysis) coupled computer code [Ref.'s 9 and 10]. Finally, a second generation finite element fluid model for the ship shock simulation of the USS JOHN PAUL JONES (DDG 53) will be presented in the Appendix.

THIS PAGE INTENTIONALLY LEFT BLANK

4

II. UNDERWATER EXPLOSIONS

A. UNDERWATER SHOCK PHENOMENA

When a high explosive, such as TNT or HBX-1 is detonated, the original solid material of the explosive is converted into a very high temperature and pressure gas within nanoseconds (on the order of 3000°C and 50000 atm.) [Ref. 11]. The pressure wave that is formed originates in one section of the explosive and propagates throughout the remainder of the explosive. As this pressure wave propagates, it initiates the chemical reaction that creates more pressure waves.
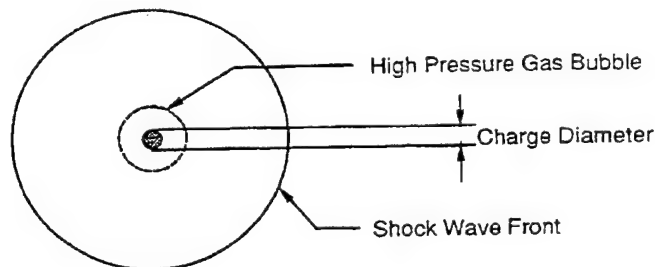
The Figure 1:Gas Bubble and Shock Wave [from Ref. 11]

The pressure wave velocity steadily increases within the solid explosive until it exceeds the speed of sound in the explosive, creating a shock wave. The shock wave propagates through the solid at a constant speed and then, with the high temperature and pressure behind the shock front, into the surrounding medium [Ref. 11]. At detonation, the pressure rise produces a steep fronted discontinuous wave, which decays exponentially with time as shown in Fig. 2. The duration of the pressure disturbance lasts only a few milliseconds. The shock wave near the charge is assumed to propagate at several times the speed of sound in water, it then falls rapidly to the acoustic velocity, approximately 5,000 ft/sec, as it travels radially outward.

5
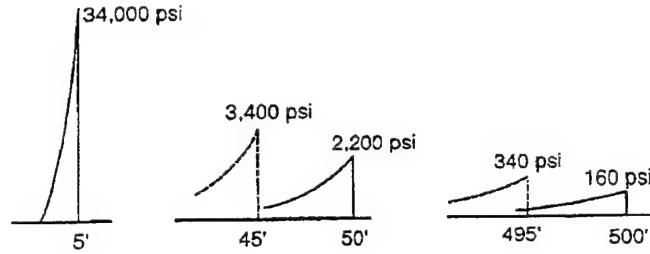
Figure 2. Shock Wave Profiles From a 300 lb. TNT Charge [from Ref. 11]

Additionally, the pressure profile of the shock wave is proportional to the inverse of the distance from the charge, $1/d$, and the wave profile gradually broadens as it spreads out [Ref. 8]. Empirical equations have been determined to define the profile of the shock wave. These relations enable calculation of the pressure profile of the shock wave ($P(t)$), the maximum pressure of the wave (P_{max}), the shock wave decay constant (θ), the bubble period (T), and the maximum bubble radius (A_{max}).

$$P(t) = P_{max} e^{-\frac{t-t_1}{\theta}} \quad \text{(psi)} \tag{2.1}$$

$$P_{max} = K_1 \left(\frac{W^{\frac{1}{3}}}{R} \right)^{A_1} \quad \text{(psi)} \tag{2.2}$$

$$\theta = K_2 W^{\frac{1}{3}} \left(\frac{W^{\frac{1}{3}}}{R} \right)^{A_2} \quad \text{(msec)} \tag{2.3}$$

$$T = K_5 \frac{W^{\frac{1}{3}}}{(D+33)^{\frac{5}{6}}} \quad \text{(sec)} \tag{2.4}$$

$$A_{max} = K_6 \frac{W^{\frac{1}{3}}}{(D+33)^{\frac{1}{3}}} \quad \text{(ft)} \tag{2.5}$$

Other variables in the equations are:

6

W = Charge weight (lbf)

R = Standoff distance (ft)

D = Charge depth (ft)

t_1 = arrival time of shock wave (msec)

t = time of interest (msec)

K_1, K_2, K_5, K_6, A_1, A_2 = Shock wave parameters

Through calculation, it can be determined that P_{max} decreases by approximately one-third after one decay constant.

The high-pressure gas that results from the explosion expands outward in a radial manner as shown in Fig. 1, and imparts an outward velocity on the surrounding water. Initially, the pressure is much greater than the atmospheric and hydrostatic pressure that opposes it and is compressive in nature. Subsequent pressure waves or bubble pulses are generated by the oscillation of the gas bubble created by the underwater explosion. The peak pressure of the first bubble pulse is approximately 10-20% of the shock wave, but is of greater duration making the area under both pressure curves similar [Ref. 11]. The inertia of the bubble causes it to expand beyond dynamic equilibrium. This means the internal pressure is less then the hydrostatic plus atmospheric. The bubble then contracts beyond dynamic equilibrium, followed by another expansion. This oscillation sequence continues until the energy of the reaction is dissipated or the bubble reaches the free surface or impacts the target. Bubble pulse excitation significantly effects the wiping response of a ships hull.

Depending on the charge location, depth of the water and bottom composition, other effects are characteristic of an underwater shock. Bottom bounce is the reflection of the shock wave off of the bottom of the body of water. If the bottom was perfectly rigid a compressive wave originating from an image charge would result. Since no bottom composition is near rigid the resulting pressure pulse is much smaller then the above assumption predicts. In reasonably deep water, this effect is not an issue for surface vessels.

7

Free surface reflection is a very important effect. The reflection of a pressure wave from a free surface results from the requirement that the pressure above the surface be unchanged, and the reflected wave must therefore be one of negative pressure. This type of pressure wave is called a rarefaction wave. This rarefaction wave causes bulk cavitation.

B.   FLUID-STRUCTURE INTERACTION

When an object such as a ship is in the vicinity of an underwater explosion, the shock pressure pulses produced by the explosion impinge upon the surface of the structure. A fluid-structure interaction takes place as the pressure pulse acts upon the flexible surface of the structure. This discretized equation of structural motion can be expressed by:

$$[M_s]\{\ddot{x}\} + [C_s]\{\dot{x}\} + [K_s]\{x\} = \{f\} \qquad (2.6)$$

where $[M_s]$ is the mass matrix, $[C_s]$ is the dampening matrix, $[K_s]$ is the stiffness matrix, $\{\ddot{x}\}$ is the acceleration vector, $\{\dot{x}\}$ is the velocity vector, and $\{x\}$ is the displacement vector of the structure and $\{f\}$ is the external force vector. In the case of a submerged structure excited by an acoustic wave, $\{f\}$ is given by:

$$\{f\} = -[G][A_f](\{p_I\} + \{p_S\}) + \{f_D\} \qquad (2.7)$$

where $[G]$ is the transformation matrix that relates the surface nodal forces of the fluid and structure, $[A_f]$ is the diagonal area matrix associated with the fluid elements, $\{p_I\}$=incident wave nodal pressure vector, and $\{p_S\}$=scattered wave nodal pressure vector [Ref. 11].

$$[M_f]\{\dot{p}_S\} + \rho c[A_f]\{p_S\} = \rho c[M_f]\{\dot{u}_S\} \qquad (2.8)$$

The approximate relation in eqn. 2.8 is called the Doubly Asymptotic Approximation (DAA) method because it approaches exactness at both low and high frequencies. This equation describes a matrix of differential equations in time for the approximation of acoustic fluid-structure interaction. The DAA represents the surrounding fluid of the

8

structure through the interaction of state variables pertaining only to the structure's wet surface. The terms of the equation are: $[M_f]$ is the symmetric fluid mass matrix for the wet-surface fluid mesh, $\{p_S\}$ and $\{\dot{p}_S\}$ are the nodal pressure vector and its first time derivative of the scattered wave, c is the acoustic velocity of water, $[A_f]$ is the diagonal area matrix associated with the fluid elements, and $\{\dot{u}_S\}$ is the scattered wave velocity vector. [Ref. 10]

The kinematic compatibility relation can then be applied to relate $\{u_S)$ to the structural response,

$$[G]^T\{\dot{x}\} = \{u_I\} + \{u_S\} \tag{2.9}$$

The "T" superscript indicates the transpose of the matrix. This equation is an expression of the constraint that the normal fluid particle velocity must match the normal structural velocity on the structure wetted surface.

Substituting Equation (2.7) into (2.6) and Equation (2.9) into (2.8) results in Equations (2.10) and (2.11),

$$[M_s]\{\ddot{x}\} + [C_s]\{\dot{x}\} + [K_s]\{x\} = -[G][A_f](\{p_I\} + \{p_S\}) \tag{2.10}$$

and

$$[M_f]\{\dot{p}_S\} + \rho c[A_f]\{p_S\} = \rho c[M_f]([G]^T\{\ddot{x}\} - \{\dot{u}_I\}) \tag{2.11}$$

The Underwater Shock Analysis (USA) code solves Eqs. (2.10) and (2.11) simultaneously by using a staggered solution procedure that is unconditionally stable with respect to the time step used [Ref. 10]. Once this system of equations is solved, desired response results such as displacement, velocity, and acceleration can be studied.

C.   CAVITATION

Two types of cavitation can occur during an UNDEX event. "Local cavitation" occurs at the fluid-structure interface and "bulk cavitation" occurs near the free surface and can cover a relatively large area.

1. Local Cavitation

Taylor flat plate theory, the simplest case of fluid-structure interaction is used to illustrate how local cavitation occurs. In this case, an infinite, air-backed plate is acted upon by an incident plane shock wave as shown below in Fig. 3.
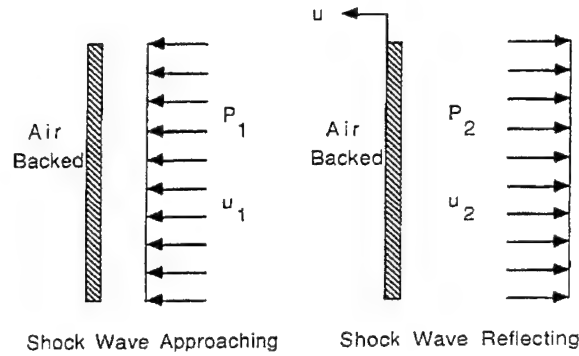
Figure 3. Taylor Plate Subjected to a Plane Wave [Ref. 9]

Once the shock wave strikes the plate, a reflected shock wave leaves the plate. According to Newton's second law of motion as shown in Eq. (2.12),

$$m\frac{du}{dt} = P_1 + P_2 \qquad (2.12)$$

where m is the mass of the plate per unit area, u is the velocity of the plate after being subjected to the shock wave, $P_1(t)$ is the incident wave pressure and $P_2(t)$ is the reflected, or scattered, wave pressure. Define the fluid particle velocities behind the incident and reflected shock waves as $u_1(t)$ and $u_2(t)$. The velocity of the plate is then defined by Eq. (2.13),

$$u(t) = u_1(t) - u_2(t) \qquad (2.13)$$

For the one dimensional plane wave, the wave equation is $P = \rho Cu$. It follows that the incident and reflected shock wave pressures, Eqs. (2.14) and (2.15), are

10

$$P_1 = \rho C u_1 \tag{2.14}$$

$$P_2 = \rho C u_2 \tag{2.15}$$

where ρ is the fluid density and C is the acoustic velocity in water. Substituting the above pressure Eqs (2.14) and (2.15) into the velocity Eq. (2.13) results in the incident shock pressure. The incident shock wave pressure is defined as Eq. (2.16)

$$P_1(t) = P_{max} e^{-\frac{t}{\theta}} \tag{2.16}$$

Solving for the reflected shock pressure yields Eq. (2.17),

$$P_2(t) = P_1 - \rho C u = P_{max} e^{-\frac{t}{\theta}} - \rho C u \tag{2.17}$$

where t is the time after the shock wave arrives at the target. Now the equation of motion, Eq. (2.12) can be rewritten as Eq. (2.18),

$$m(\frac{du}{dt}) + \rho C u = 2 P_{max} e^{-\frac{t}{\theta}} \tag{2.18}$$

which is a first order, linear differential equation. The solution, u(t), of the differential equation is expressed in Eq. (2.19) as

$$u = \frac{2 P_{max} \theta}{m(1-\beta)} [e^{-\frac{\beta t}{\theta}} - e^{-\frac{t}{\theta}}] \tag{2.19}$$

with $\beta = \rho C \theta / m$ and t>0. The total pressure that impinges on the plate is defined as Eq. (2.20),

$$P_1 + P_2 = P_{max} [\frac{2}{1-\beta} e^{-\frac{t}{\theta}} - \frac{2\beta}{1-\beta} e^{-\frac{\beta t}{\theta}}] \tag{2.20}$$

As the value of β becomes larger, as in the case of a lightweight plate, the total pressure will become negative at a very early time. However, since water cannot support tension, negative pressure cannot exist. Therefore, as the water pressure reduces to vapor

pressure at the surface of the plate, cavitation occurs. At this point, the pressure in front of the plate has been cut off and the plate has reached its maximum velocity. [Ref.12]

A ship's hull can be easily generalized as a Taylor flat plate. Local cavitation is likely to occur along the hull where the pressure pulse from the UNDEX impinges with sufficient force and the hull plating β value is large enough to make the net pressure negative.

2. Bulk Cavitation and Vertical Kick-off Velocity

As detailed above, a rarefaction wave, which is tensile in nature, is created when the shock wave is reflected from the free surface. Since water cannot sustain a significant amount of tension, cavitation will occur when the pressure drops to zero or below. Upon cavitation, the water pressure rises to the vapor pressure of water, approximately 0.3 psi. This cavitated region created by the rarefaction wave is known as the bulk cavitation zone. It consists of an upper and lower boundary and its extent is dependent on the charge size, type, and depth [Ref.'s 11 and 12].

Figure 4 shows a typical bulk cavitation zone. The cavitation zone is symmetric about the y-axis in the figure. The water particles behind the shock wave front at the time of cavitation have velocities depending on their location relative to the charge and the free surface. Water particles near the free surface, for example, will have a primarily vertical velocity at cavitation. As the reflected wave passes, the particles will be acted upon by gravity and atmospheric pressure.

An estimate of the vertical kick-off velocity of a surface ship can be arrived at by looking at the fluid particle velocities near the free surface. Since the mass of the ship is the same as the water it displaces, the water particle velocities through this volume can be calculated to give the ships velocity. The centerline can be calculated and used as the average vertical kickoff velocity of the ship section. [Ref. 12]

The upper cavitation boundary is the set of points where the rarefaction wave passes and reduces the absolute pressure to zero or a negative value. The region will remain cavitated as long as the pressure remains below the vapor pressure. The total or absolute pressure, which determines the upper boundary, is a combination of atmospheric

12

pressure, hydrostatic pressure, incident shock wave pressure, and rarefaction wave pressure.
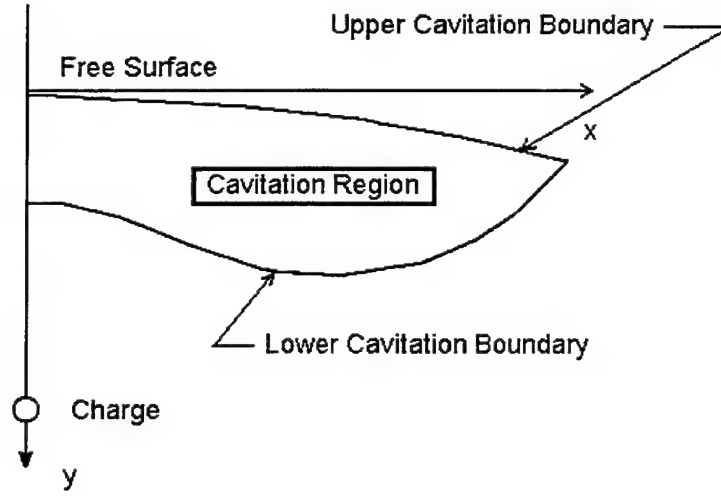
Figure 4. Bulk Cavitation Zone [Ref. 12]

The lower cavitation boundary is determined by equating the decay rate of the breaking pressure to the decay rate of the total absolute pressure. The breaking pressure is the rarefaction wave pressure that reduces a particular location of a fluid to the point of cavitation pressure, or zero psi.

The upper and lower cavitation boundaries can be calculated from Equations (2.21) and (2.22), respectively [Ref. 12]. Any point which satisfies F(x,y) and G(x,y) = 0 determines the bulk cavitation boundary.

$$F(x,y) = K_1\left(\frac{W^{\frac{1}{3}}}{r_1}\right)^{A_1} e^{\frac{(r_2 - r_1)}{\theta}} + P_A + \gamma y - K_1\left(\frac{W^{\frac{1}{3}}}{r_2}\right)^{A_1} \tag{2.21}$$

$$G(x,y) = -\frac{P_i}{C\theta}\left\{1 + \left[\frac{r_2 - 2D\left(\frac{D+y}{r_2}\right)}{r_1}\right]\left[\frac{A_2 r_2}{r_1} - A_2 - 1\right]\right\} - \tag{2.22}$$

$$\frac{A_1 P_i}{r_1^2}\left[r_2 - 2D\left(\frac{D+y}{r_2}\right)\right] + \gamma\left(\frac{D+y}{r_2}\right) + \frac{A_1}{r_2}\left(P_i + P_a + \gamma y\right)$$

13

The variables in Equations (2.21) and (2.22) are:

x, y = horizontal range and vertical depth of the point

r_1 = standoff distance from the charge to the point

r_2 = standoff distance from the image charge to the point

C = acoustic velocity in the water

D = charge depth

θ = decay constant

γ = weight density of water

P_A = atmospheric pressure

W = charge weight

P_i = P(t), Equation (2.1)

θ = Equation (2.3)

K_1, A_1 = shock wave parameters

Figure 5 shows the charge geometry for the above two equations.
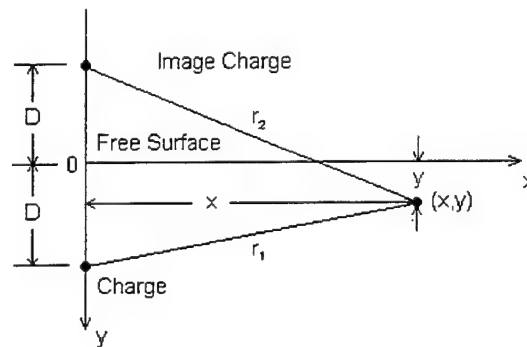
Figure 5. Charge Geometry for Bulk Cavitation Equations [Ref. 12]

14

Appendix A provides a MATLAB m-file that calculates and plots the bulk cavitation zone for a user supplied charge weight and depth by solving Equations (2.21) and (2.22).

THIS PAGE INTENTIONALLY LEFT BLANK

III. PREVIOUS NPS UNDEX RESEARCH

Significant work in the area of surface ship modeling and simulation has been accomplished at the Naval Postgraduate School. The work of Santiago [Ref. 14] and Wood [Ref. 13] provided the background experience and modeling techniques that led to promising results in the modeling and simulation of the ship shock trial of USS John Paul Jones (DDG-53) as presented in Ref. 7.

Subsequent developments in the modeling and simulation codes utilized in Ref.'s 13 and 14 have greatly simplified these tasks. To illustrate the streamlining of the modeling and simulation process consider the number of different computer codes utilized in the previous work. In Ref. 14, Santiago used 2 modeling codes, 6 analysis codes and 4 post-processors. In Ref. 13, Wood used 2 modeling codes, 3 analysis codes and 4 post-processors. This study uses 1 modeling code, 2 analysis codes and 2 post-processors.

A. ONE-DIMENSIONAL MODEL

Santiago in Ref. 14 offered an example of a one-dimensional problem involving the interaction between an air-backed plate and a cavitating fluid. This analysis utilized the USA-CFA (Underwater Shock Analysis-Cavitating Fluid Analyzer) [Ref. 15] code to solve this problem. The excitation is from a plane exponential wave impinging upon the plate. H.H. Bleich and I.S. Sandler, describe an exact solution to this problem [Ref. 16]. Ref. 14 produced identical results as those shown by Bleich and Sandler.

The method utilized by Santiago has been greatly simplified due to subsequent development of the USA and LS-DYNA codes. The one-dimensional model was constructed using the TrueGrid mesh generation code. All nodes in the model are constrained allowing only freedom in the X (vertical) direction. The model represents an air-backed plate at the free surface of a cavitating fluid. The structural plate is modeled by a single 1.5-in square shell element. The structure was constructed of 1-in steel plate modeled by LS-Dyna material Type 1:Mat_Elastic (weight density of 0.284-lbf/in^3, Young's Modulus of 30E6-psi and Poison's Ratio of 0.3) [Ref. 9]. The fluid column is

17

modeled by 100 hexahedral solid elements and contains 404 nodes. The fluid is modeled by LS-Dyna material Type 90:Mat_Acoustic (weight density of 0.0361-lbf/in^3, acoustic speed of 4760-ft/sec) [Ref. 9]. The fluid volume was constructed using the TrueGrid's BLUDE command. This command extrudes a set of polygons through the mesh lines of a user-defined block (grid) [Ref. 8]. The USA and LS-DYNA input decks used for this model are contained in Appendix B. Figure 6 shows the model geometry. The DAA1 boundary for this model is defined at the bottom of the fluid column.
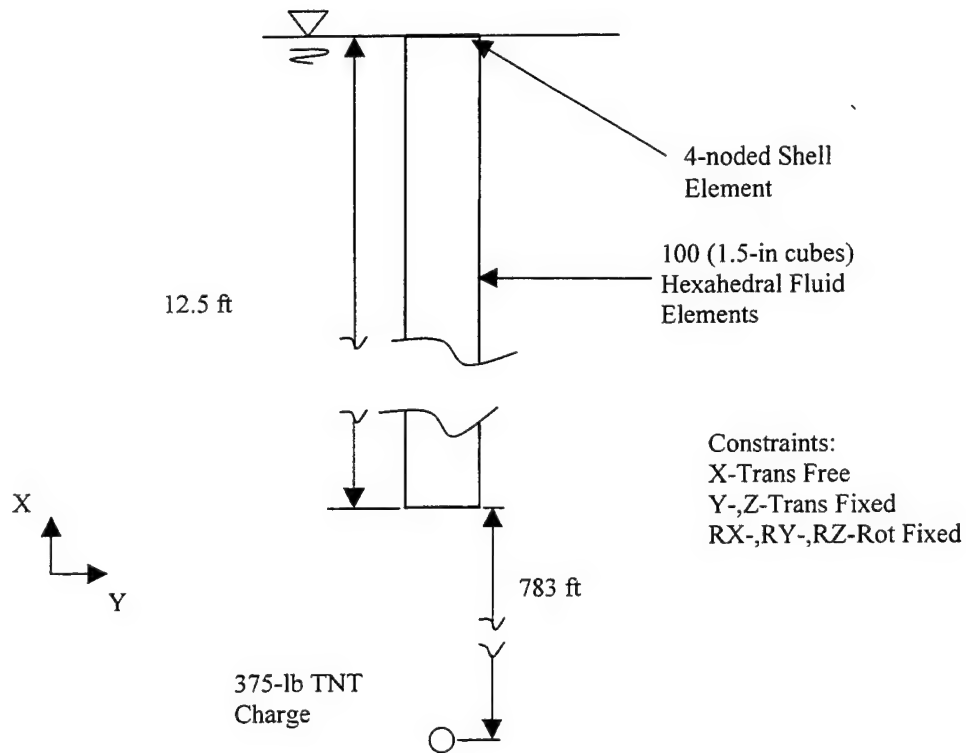
Figure 6: 1D Plate and Cavitating Fluid Model

B. TWO-DIMENSIONAL MODEL

Wood in Ref. 13 investigated the effect of cavitation on a ship-like box structure subjected to an UNDEX event. The study looked at two- and three-dimensional models and compares the effect of modeling with and without a coupled fluid volume. Additionally, Ref. 13 investigates the effects of toggling the LS-Dyna material Type

90:Mat_Acoustic cavitation flag on and off and Rayleigh damping. The LS-Dyna and USA input decks for the present study are based largely on those developed in Ref. 13.

Wood in Ref. 13 presents a two-dimensional model to perform the initial analysis and verify the shock wave behavior in the fluid mesh. The two-dimensional model consists of a midships section of a ship-like box structure and a surrounding fluid volume. A similar model is presented here to illustrate the shock wave propagation in the models.

The two-dimensional model was constructed using the TrueGrid mesh generation code. The structural model represents a cross-sectional area of a barge. It is 24-in wide, 24-in high and 6-in deep. It contains two symmetric boundary conditions on the XY-planes. The shell plating was constructed of ¼-in steel plate modeled by LS-Dyna material Type 1:Mat_Elastic (weight density of 0.284-lbf/in³, Young's Modulus of 30E6-psi and Poison's Ratio of 0.3) [Ref. 9]. The finite element mesh of the barge structure contains 38 nodes and 18 shell elements. The fluid volume is 80-in wide, 120-in high and 6-in deep. The fluid is modeled by LS-Dyna material Type 90:Mat_Acoustic (weight density of 0.037-lbf/in³, acoustic speed of 4929.6-ft/sec) [Ref. 9]. The fluid volume was constructed using the TrueGrid's BLUDE command. The finite element mesh of the fluid volume contains 616 nodes and 270 hexahedral solid elements. Figure 1 shows the fluid volume finite element model.

Of particular importance in 2D models utilizing the USA code is the numbering of nodes along the DAA1 boundary. This boundary is located around the circumference of the fluid mesh. For example, the DAA1 boundaries are the faces parallel to the Z axis in figure 10, excluding the free surface. Referring to figure 8 and imagining the 2D cross-section as a cylinder section, the first two nodes of these DAA1 face elements should progress around the circumference not along the Z axis. The NSORDR command in the USA FLUMAS input deck allows the user to cyclically reorder these nodes to achieve this requirement [Ref. 17]. See the 2D USA FLUMAS input deck in Appendix B.
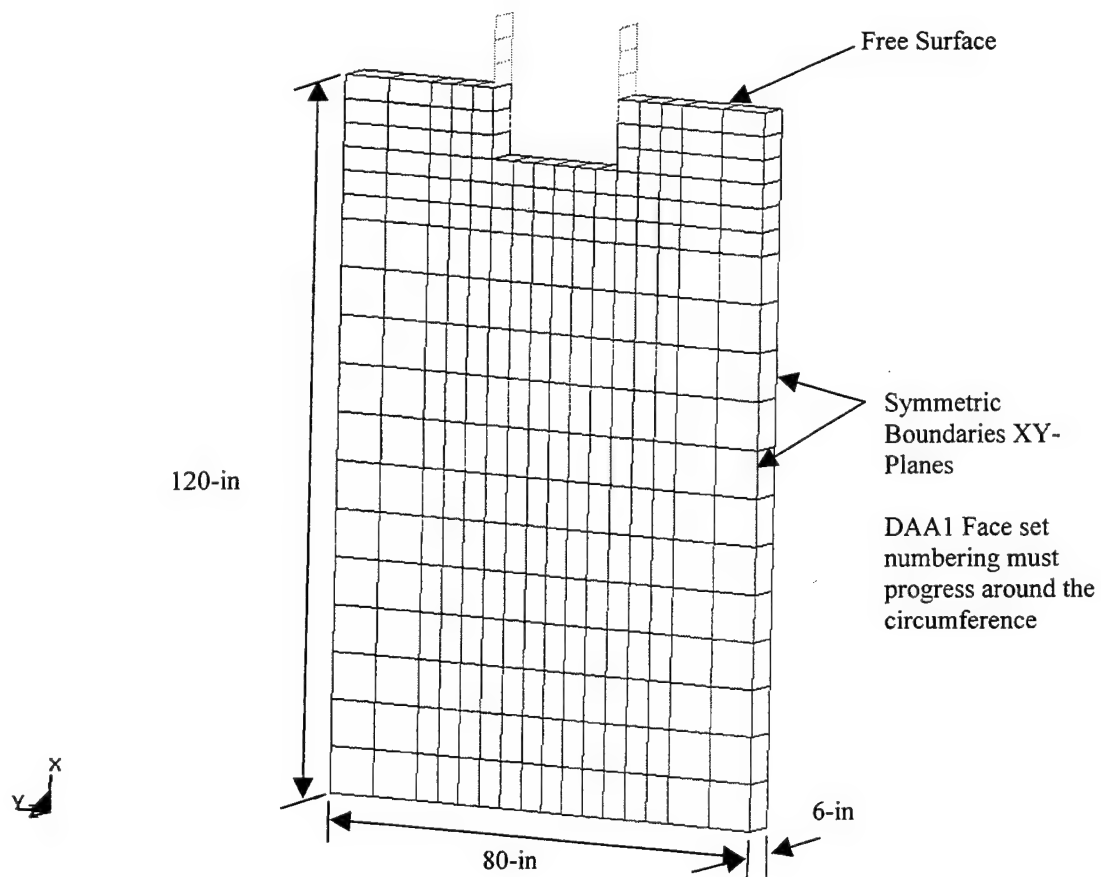
Figure 7: 2-D Fluid Model with Barge Cross-section

Free Surface

Symmetric Boundaries XY-Planes

DAA1 Face set numbering must progress around the circumference

120-in

80-in

6-in
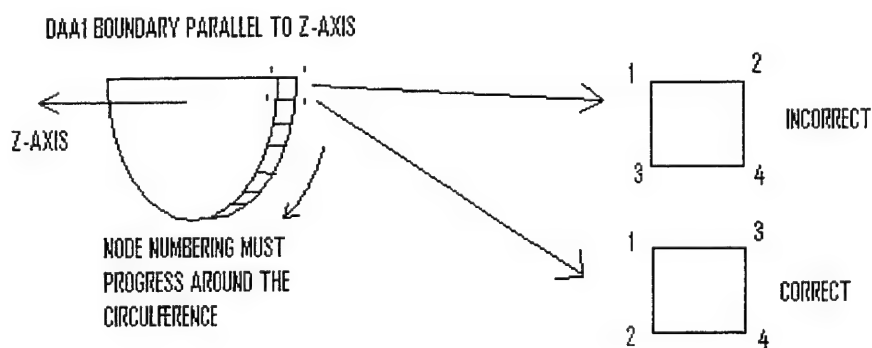
Figure 8: 2D Faceset Node Numbering

DAA1 BOUNDARY PARALLEL TO Z-AXIS

Z-AXIS

NODE NUMBERING MUST PROGRESS AROUND THE CIRCULFERENCE

INCORRECT

CORRECT

IV. MODELING AND SIMULATION

Modeling and simulation involves model construction and pre-processing, analysis and solution, and post-processing programs. A flow chart of the model building and testing procedure is shown below in Figure 9.

Model Construction
Pre-Processing

Analysis

and

Solution

Post-Processing

Model Construction Pre-Processing	**True***Grid*®
	LS-DYNA
Analysis and Solution	**USA** FLUMAS AUGMAT TIMINT
Post-Processing	**LS-Post** **Excel**
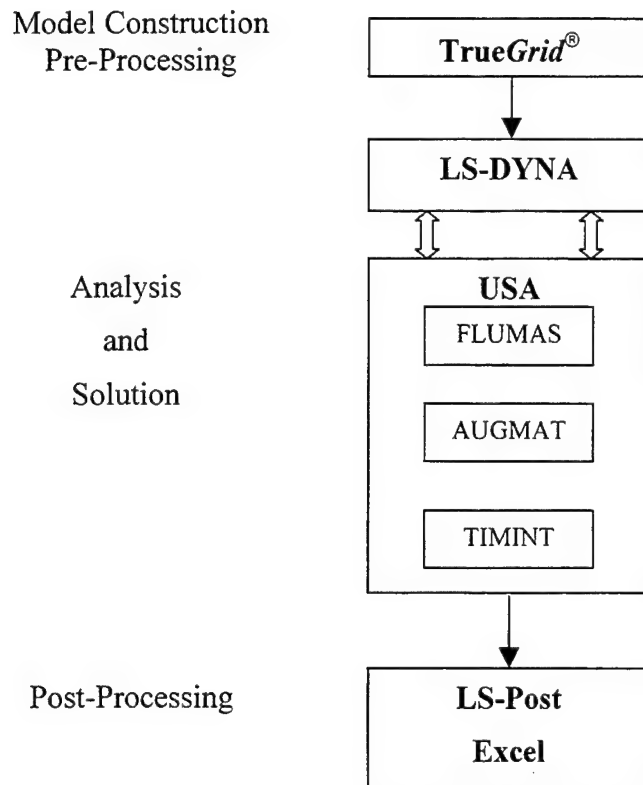
Figure 9: Flow Chart. Model Construction and Simulation

A. MODEL CONSTRUCTION AND PRE-PROCESSING

1. 3D Structural Model

The three-dimensional model was constructed using the TrueGrid mesh generation code[Ref. 8]. The structural barge model is 168-in long, 24-in wide, and 24-in deep. It contains two structural athwartships bulkheads. The model was loaded with three lumped masses (0.664-lbf s^2/in^4) evenly spaced on the centerline to give the model a 12-in waterline. The shell plating was constructed of ¼-in steel plate modeled by LS-DYNA material Type 1:Mat_Elastic (weight density of 0.284-lbf/in^3, Young's Modulus of 30E6-psi and Poison's Ratio of 0.3)[Ref. 9]. The finite element mesh of the barge structure contains 443 nodes and 432 shell elements. Figure 10 shows the barge finite element model.
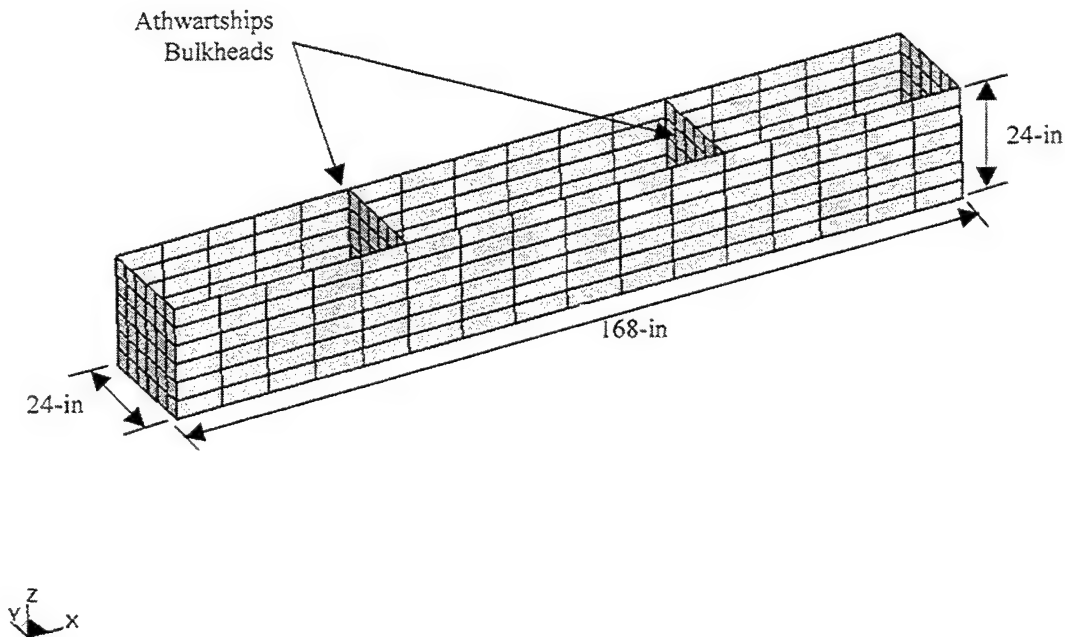
Figure 10: Barge Finite Element Model

2. 3D Fluid Modeling

The fluid is modeled by LS-DYNA material Type 90:Mat_Acoustic (weight density of 0.037-lbf/in^3, acoustic speed of 4929.6-ft/sec). The fluid volume was constructed using the TrueGrid's *BLUDE* command. This command extrudes a set of polygons through the mesh lines of a user-defined block (grid). Figure 11 shows an example of one of the fluid volume finite element models used in this study. The finite element mesh of this fluid volume contains 18615 nodes and 16272 hexahedral solid elements.

The nodal spacing adjacent to the structural model is critical for the stability of the USA analysis. The nodal distance normal to the structural mesh limits the size of the first layer of fluid elements [Ref. 15]. This parameter is determined by the following equation:

$$\frac{2D\rho}{\rho_s t_s} \leq 5$$

Where ρ = density of water, D = thickness of the fluid element in the direction normal to the wetted surface of the structure, ρ_s = density of the submerged structure, and t_s = thickness of the submerged structure. For the barge model the critical element thickness, D, is 4.8 inches. The first layer of fluid mesh for these models was set to 4-in. The bulk fluid elements were generated using the *RES* and *AS* commands. These commands space the nodes of a mesh so that the ratios of the distances between them will be constant [Ref. 8]. This means the fluid elements gradually increase in size as you move away from the structure. These commands were used to generate a consistent mesh quality at a given distance from the structure. The length and width of each fluid volume are identical. The depth of each model is varied from 324-in in the Base model to 42-in in the Third model. Table 1 summarizes the specifics of each model. Figure 12 shows the truncation of the fluid volume for the Base, Extended, Full and Half models.

This thesis also presents a second-generation coupled structural-fluid model of the USS JOHN PAUL JONES (DDG53). A detailed description of the DDG53 model is contained in Appendix D.

Table 1:Fluid Volume Models Specifics

Model	Mesh Z-dimension	Number of Nodes	Number of Fluid Elements
Base	312-in	23277	20592
Extended	144-in	18615	16272
Full	96-in	17061	14832
Half	66-in	13176	11232
Third	42-in	8414	6912
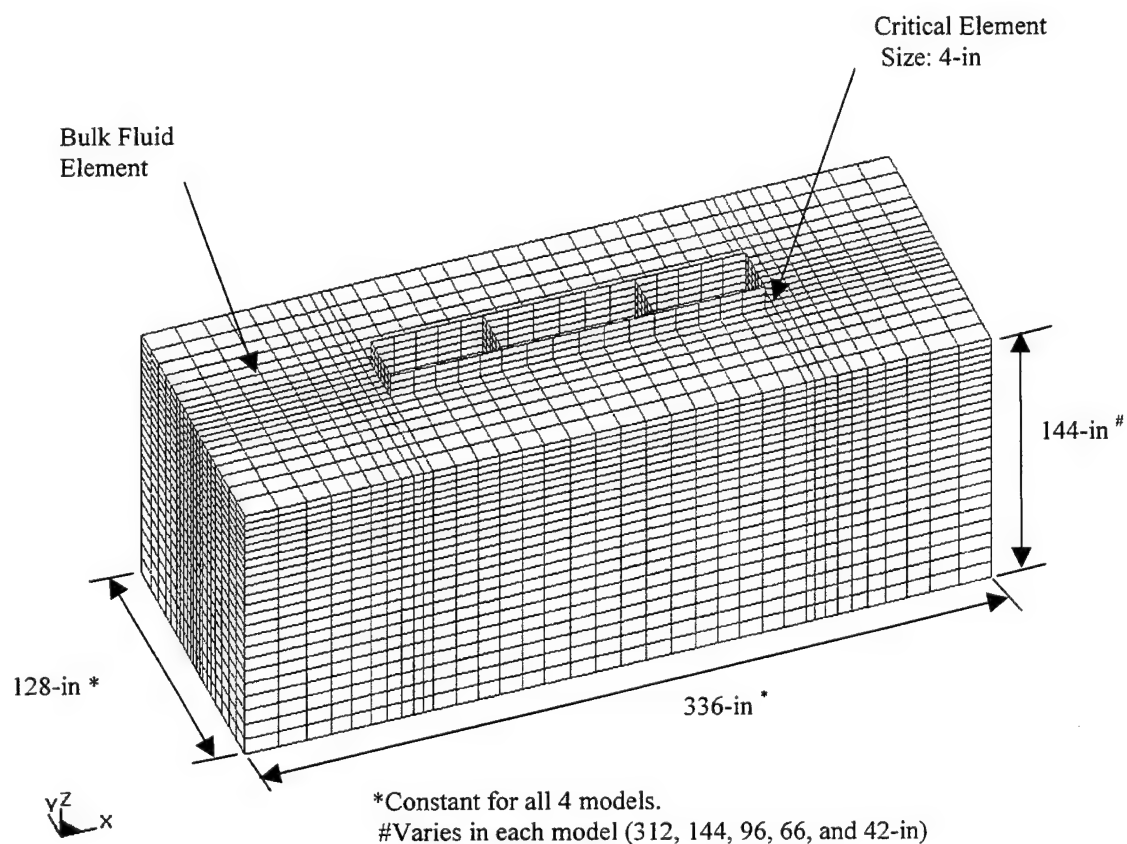
Figure 11: Example of Fluid Volume Finite Element Model

Base Model · Full Model · Extended Model · Half Model
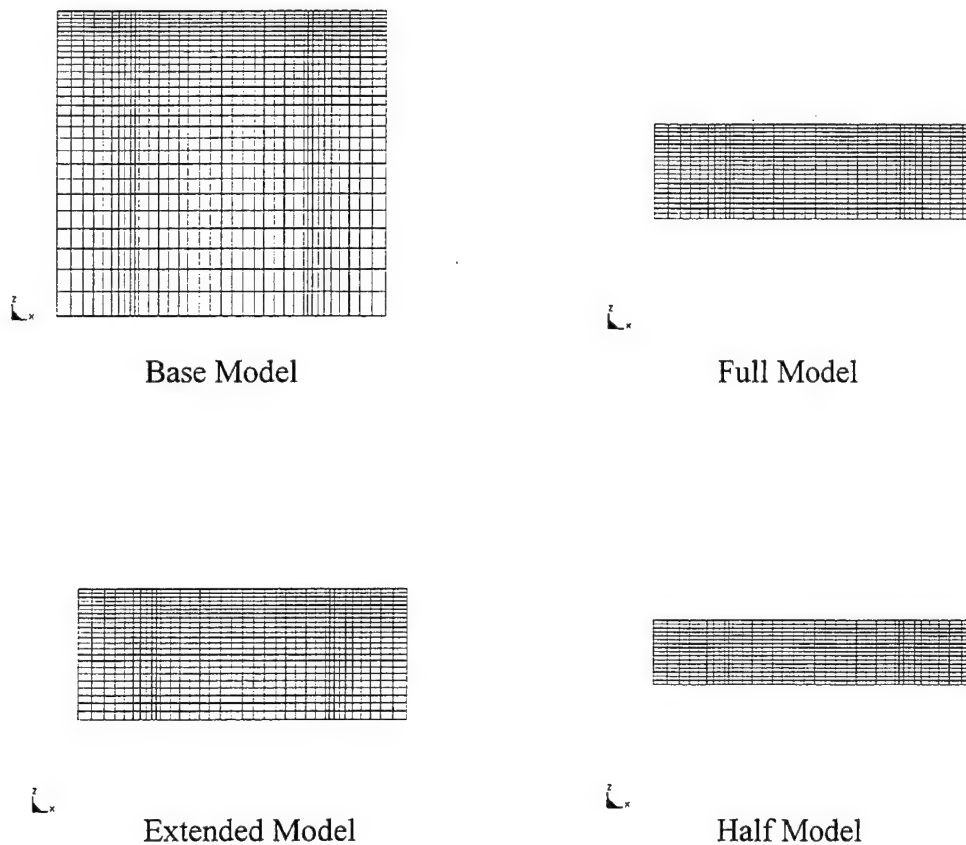
Figure 12: Fluid Volume Truncation

B. ANALYSIS AND SOLUTION

1. Analysis Program Description

The finite element model must be translated into LS-DYNA keyword format using the TrueGrid Output translator. The USA code performs the majority of the work (formulation of the fluid-structure interaction matrices) and LS-DYNA is used to perform the time integration solution for the structure. LS-DYNA is a non-linear three-dimensional structural analysis code [Ref. 9]. The USA code consists of three main modules: FLUMAS, AUGMAT, and TIMINT [Ref. 10].

FLUMAS is the first USA module required to be run. FLUMAS generates the fluid mass matrix for the submerged portion of the structure. The fluid mesh data, as well

as the transformation coefficients that relate both the structural and fluid degrees of freedom on the wetted surface are generated, including the nodal weights for the fluid element pressure forces and the direction cosines for the normal pressure force. The fluid area matrix is diagonal and the fluid mass matrix is fully symmetric.[Ref. 10]

AUGMAT is the second module to be run. This module takes the data generated by the FLUMAS and initial LS-DYNA runs to construct specific constants and arrays utilized in the staggered solution procedure for the actual transient response analysis [Ref. 14]. The AUGMAT module organizes this information so that the integrator need refer to only one permanent data file for input. The augmented interaction equations are formed from Equations (2.10) and (2.11). [Ref. 10]

TIMINT performs the direct numerical time integration and also handles the computation of the UNDEX parameters, such as the shock wave pressure profile. The structural and fluid response equations are solved separately at each time step through the extrapolation of the coupling terms for the two systems. LS-DYNA is used to solve the structural equations and the TIMINT run solves the fluid equations. A result of using the staggered solution procedure mentioned previously is that LS-DYNA and TIMINT can each have a different time step assigned. However, the general practice is to use the same time step in both computations. Despite using an unconditionally stable solution scheme, the TIMINT time step must be set small enough to accurately capture the fluid system response. Additionally, it should be mentioned that LS-DYNA uses a central-difference integration method, which is conditionally stable. The LS-DYNA time step must be less than or equal to the critical time step for the structural finite element mesh or numerical instability will result. [Ref.'s 9 and 10]

Appendix B provides example input decks for each of the three USA modules as well as an example LS-DYNA Keyword input deck.

2. 1D Model

Figure 13 shows the pressure time history of the fluid element immediately below the plate for the 1D case. The plots show the Cavitation flag on and flag off cases. These

results show excellent correspondence with those in Ref. 14 and Ref. 16. This confirms the validity of the abbreviated modeling and simulation techniques.

Pressure

Vertical Velocity
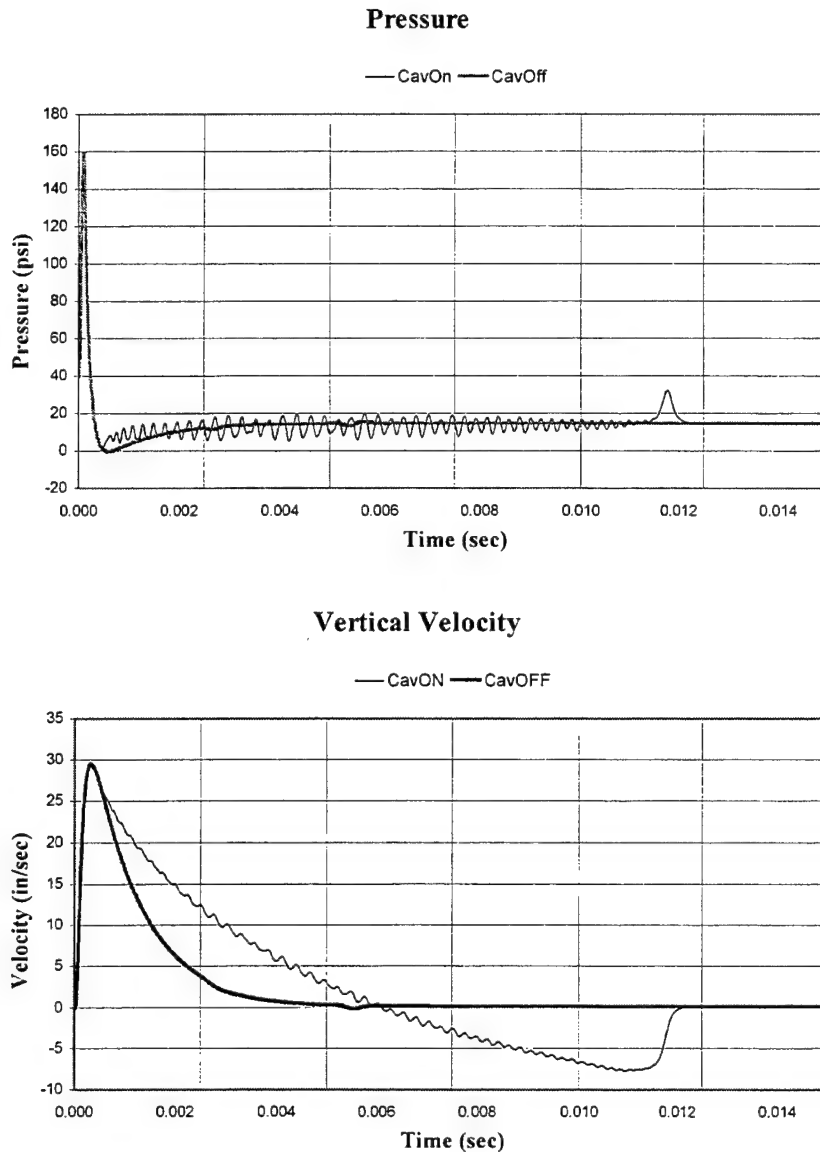
Figure 13: Pressure and Velocity Response of 1D Model

3. 2D and 3D Test Description

The charge placement, designated SHOT-1, used in the shock simulation run for the 2D and 3D models in this study was a port side beam on shot. A 60 lb. TNT charge

27

was selected for the simulations. SHOT-1 placed the charge offset from the side of the barge at a horizontal standoff distance of 10-ft (120-in) and a depth of 25-ft (300-in) from the free surface. The coordinate location of the charge was (84,-132,-288-in). Figure 14 shows this attack geometry and Table 2 shows a summary of the UNDEX parameters of the explosion. As listed in Table 2, the bubble period is over 500-msec so there is no bubble interaction in the 50 msec run-time of this study. Figure 15 shows the theoretical pressure profile at the barge for this shot geometry. The times listed in Figure 15 are taken from the instant of detonation. The bulk cavitation zone was computed and is shown in Figure 16. The theoretical depth of the cavitation under the barge structure is 84-in. Since the mass of the surface ship is the same as the water it displaces, an estimate of the vertical kick-off velocity of the ship can be found based on the water particle velocities [Ref. 12]. For the geometry of SHOT-1 the theoretical kick-off velocity was calculated as 20.7-ft/sec.
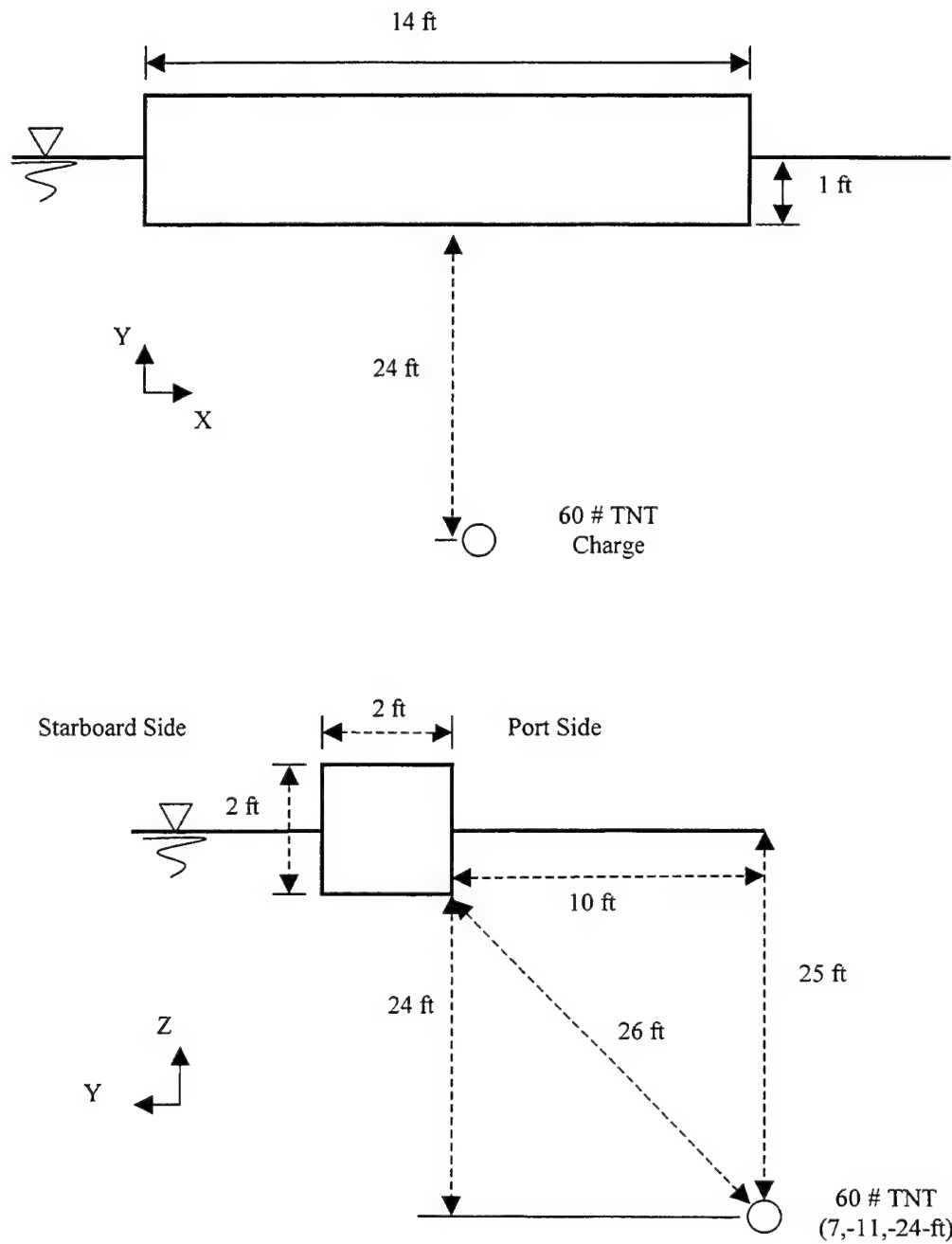
Figure 14: SHOT-1 Geometry

Table 2: UNDEX Parameters

Radial Standoff	312.0 in
P_{max}	2409 psi
θ	0.322 msec
T	0.567 sec
A_{max}	153.70 in

29

Theoretical Pressure Profile
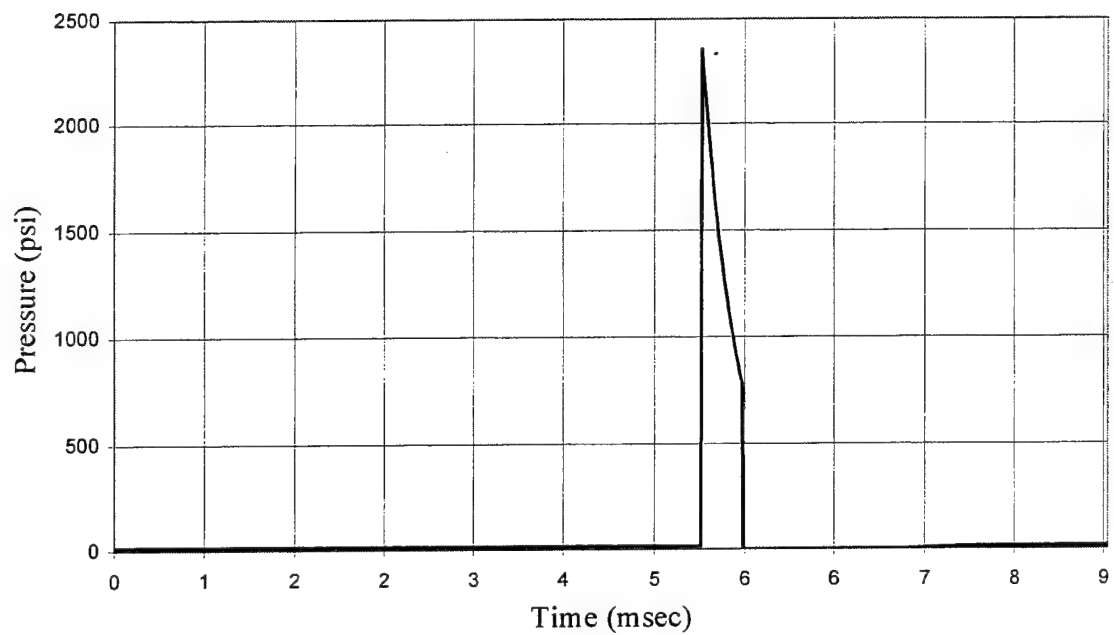
Figure 15: Theoretical Pressure Profile for SHOT-1

Theoretical Bulk Cavitation Zone
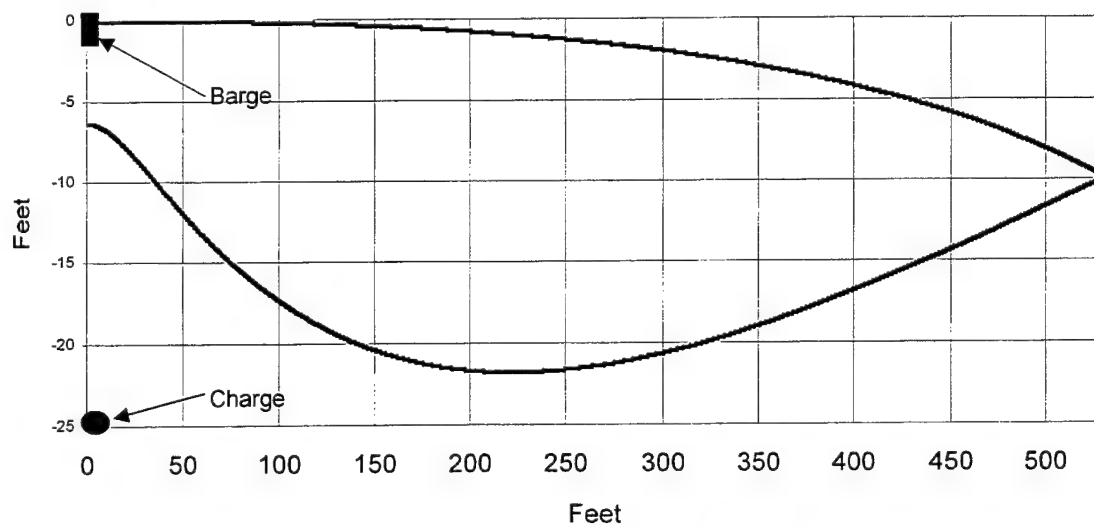
Figure 16: Cavitation Zone for SHOT-1

30

4. 2D Model Results

The pressure time histories of three fluid elements are plotted in figure 17. These elements represent the fluid pressure in the top, middle and bottom of the coupled fluid volume. The magnitude and decay of these plots matches what is expected from the geometry of the UNDEX attack. The second peaks seen are due to the reflection of the incident shock wave off the structure. The cut off of the pressure in the top and middle elements represents cavitation. The bottom element does not experience this cut off indicating no cavitation at this depth. This confirms the proper behavior of the model since the theoretical cavitation depth was 84-in. Figure 18 shows the incident shock wave in the 2D fluid mesh.
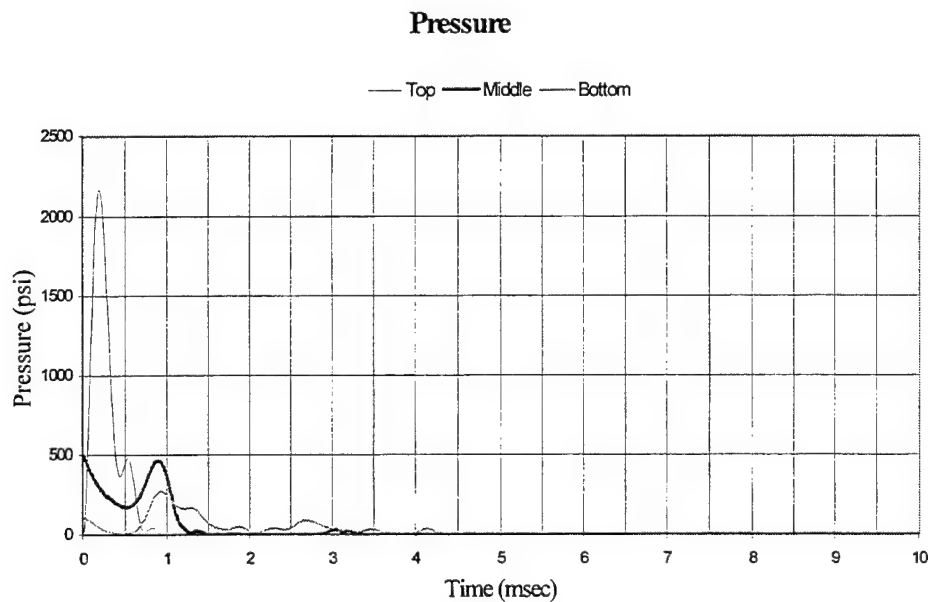
Pressure

Figure 17: 2D Pressure Response

Time =   0
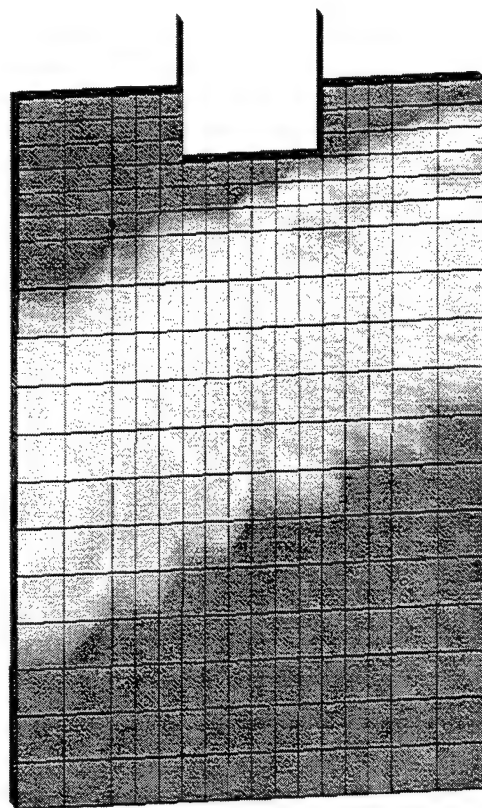
Figure 18: 2D Incident Shock Wave

C.   POST-PROCESSING

The solution data is output into two formats for analysis: binary and ASCII. The binary data files created by the LS-DYNA/USA runs contain the model's finite element response information.   LS-POST [Ref 18] was used for three-dimensional response visualization.   It provides animation and image generation features.   This allows the animation of the shock wave propagation through the fluid to the structure.   Additionally, LS-POST has the capability of extracting ASCII solution data, plotting time histories of fluid and structural responses (pressure, stress, velocity, acceleration, etc.) and writing it to a separate ASCII file for later evaluation.   The Time history plots were made by exporting the LS-POST data to Excel.

THIS PAGE INTENTIONALLY LEFT BLANK

V. 3D SIMULATION RESULTS

This study examined the effect of decreasing the fluid mesh depth on the nodal response of the barge structure. The five fluid models studied were explained above and are simply labeled Base, Extended, Full, Half and Third. The nodes analyzed are listed in Table 3 and shown in Figure 19. These nodes were chosen based on their physical location in the structure.

Table 3: Response Nodes Coordinates

Node	25	159	213	285	398
x,y,z Coordinate (inches)	(0,0,12)	(50,0,12)	(84,0,0)	(118,12,12)	(142,12,12)
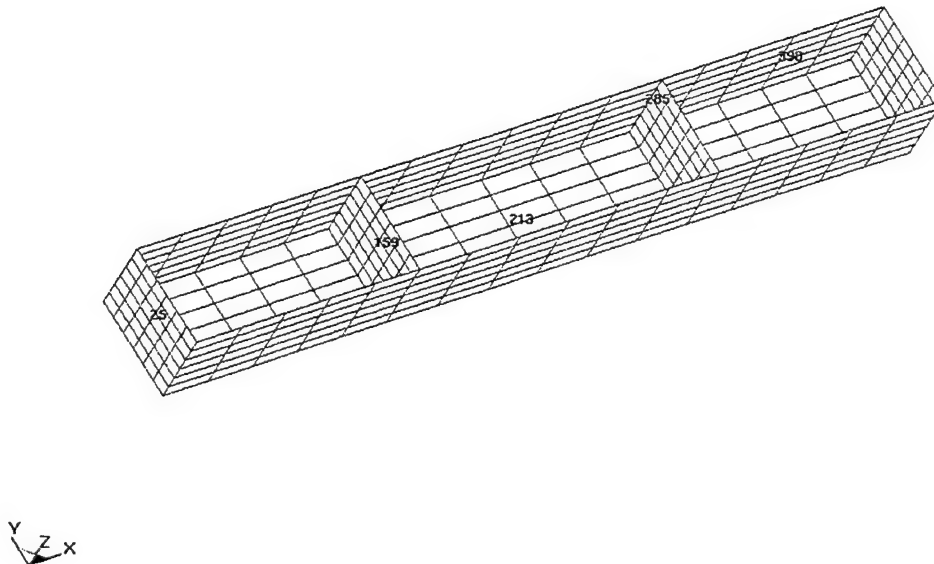
Figure 19: Nodes Analyzed

The vertical response of the selected nodes are calculated and compared for the five fluid volume models. The Base model is used as a reference for the comparisons. The time history plots of the Base and Third models for the selected nodes are offered as an example of the response data. Although they were developed to compare measured verse calculated data, the Russel and updated Geers error measurement criteria are adapted in this study to quantify the effect of truncating the fluid volume depth [Ref.'s 19, 20 and 21]. The formulation of these error factors is shown below.

$$\psi_{cc} = T^{-1} \int_0^T f_1^2(t)dt \qquad\qquad GM = \sqrt{\psi_{cc}/\psi_{mm}} - 1$$

$$\psi_{mm} = T^{-1} \int_0^T f_2^2(t)dt \qquad\qquad GP = 1 - \psi_{cm}/\sqrt{\psi_{cc}\psi_{mm}}$$

$$GC = \sqrt{RM^2 + RP^2}$$

$$\psi_{cm} = T^{-1} \int_0^T f_1(t)f_2(t)dt$$

Updated Geers Error Formulation [Ref. 21]

$$A = \sum_{i=1}^N f_1(i)^2 \qquad\qquad P = C/\sqrt{AB}$$

$$B = \sum_{i=1}^N f_2(i)^2 \qquad\qquad RP = \cos^{-1}(P)/\pi$$

$$RM = \operatorname{sign}(m)\log_{10}(1 + |m|)$$

$$m = (A - B)/\sqrt{AB}$$

$$RC = \sqrt{\pi/4 \left(RM^2 + RP^2\right)}$$

$$C = \sum_{i=1}^N f_1(i)f_2(i)$$

Russel Error Formulation [Ref. 19]

The tabulated results of the magnitude, phase and comprehensive error factors are presented. The Russel error factors are designated **RM, RP** and **RC**. Reference [19]

36

suggests if the magnitude, phase and comprehensive Russel error factors are less then 0.2 the correlation between the data is acceptable. However, since this is a sensitivity analysis of simulation models a factor of 0.1 is used. The updated Geers error factors are designated **GM**, **GP** and **GC**.

Theoretical and Simulation Pressure Profile
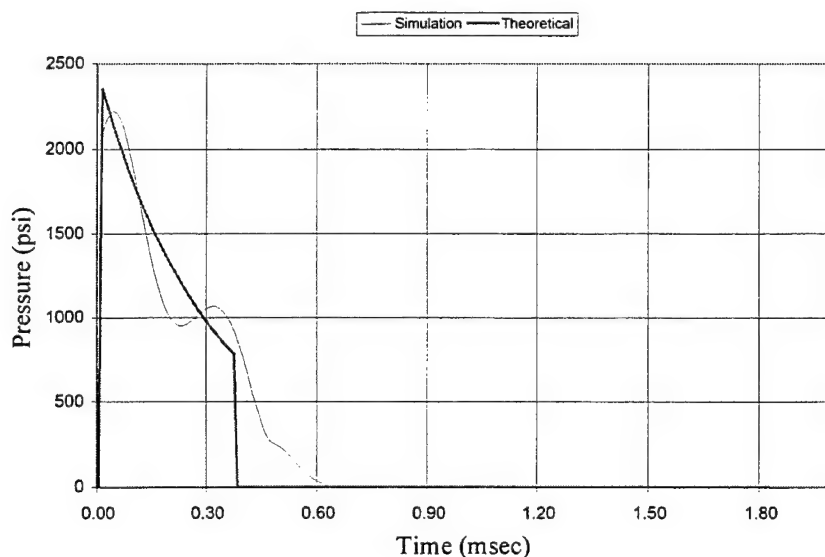
Figure 20: Resulting Pressure Profile at Midships of Barge

A. INCIDENT SHOCK WAVE AND BULK CAVITATION FORMATION

Figure 19 shows the theoretical and simulation results pressure-time history of fluid (brick) element 2239 of the Base model. This element is located on the port side of the structure at coordinate (84,-16,-4). This pressure profile is typical of all four models and compares well to the theoretical profile. As seen in Figure 19, the pressure rises quickly to a peak, dips and then peaks again at approximately 0.35-msec. This second peak is due to reflection of the incident pressure wave off the structural model. The pressure drops off to zero at 0.6-msec representing cavitation. This pressure-time response shows reasonable correlation with the 2D model presented above. Figures 21-25 show the incident shock (fig. 21), initial cavitation bubble formation (fig. 22-23) and

37

complete envelopment of the barge by bulk cavitation (fig 24-25). Figures 22 and 23 are at time 0.4-msec and figures 24 and 25 are at time 1.09-msec. These events correspond well with the pressure-time history of figure 19.

Time - 0
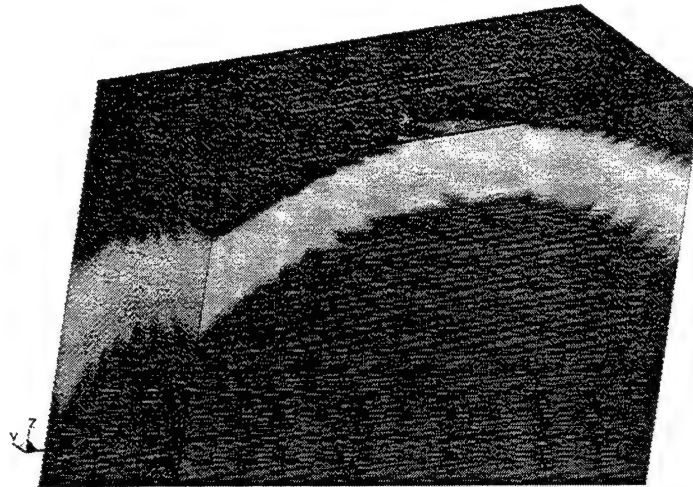
Figure 21: Incident Shock Wave

Time - 0.0004
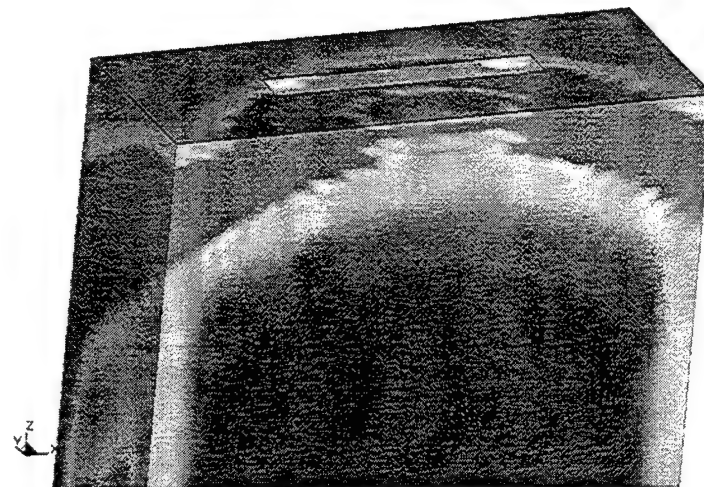
Figure 22: Initial Bulk Cavitation Zone

Time = 0.0004
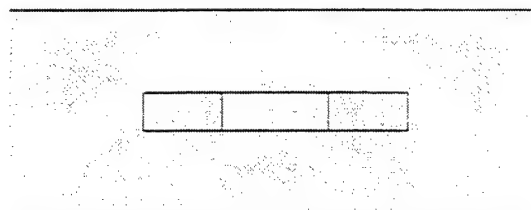
Figure 23: Top View of Initial Bulk Cavitation Zone

Time = 0.00101
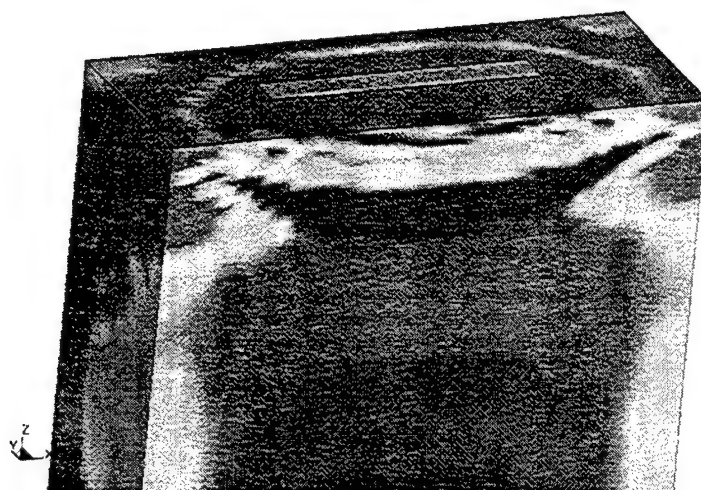
Figure 24: Barge Enveloped by Bulk Cavitation

Time = 0.0003

Y
L x
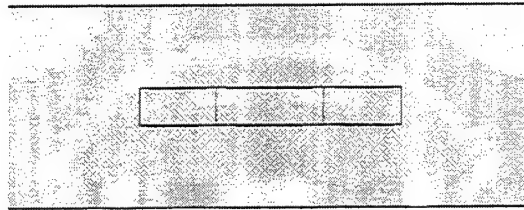
Figure 25: Top View of Barge Enveloped by Bulk Cavitation

B. VERTICAL VELOCITY RESPONSE

Figure 26 shows the vertical bodily response of the barge model to the UNDEX attack. The results plotted represent the vertical velocity of the barge structure from the time of impact of the incident UNDEX shock wave out to 50-msec. The response is as expected from the physics of the attack. The incident shock wave impacts the structure with extremely high pressure and forces the barge rapidly upward. This initial velocity of approximately 21 ft/sec corresponds well to the theoretical kickoff velocity of 20.7 ft/sec. The velocity continues to increase until approximately 1-msec, the onset of bulk cavitation. At 4-msec the velocity of the structure hits the peak value, approximately 23-ft/sec. The barge velocity then drops off and becomes negative at 45-msec. The oscillations in the time history are due to the dynamic structural response, such as bending and torsional modes, of the barge. (For an insight into the effect of the coupled fluid volume, see Appendix E for a comparison of coupled verse uncoupled model responses).

40

Overall Vertical Bodily Response
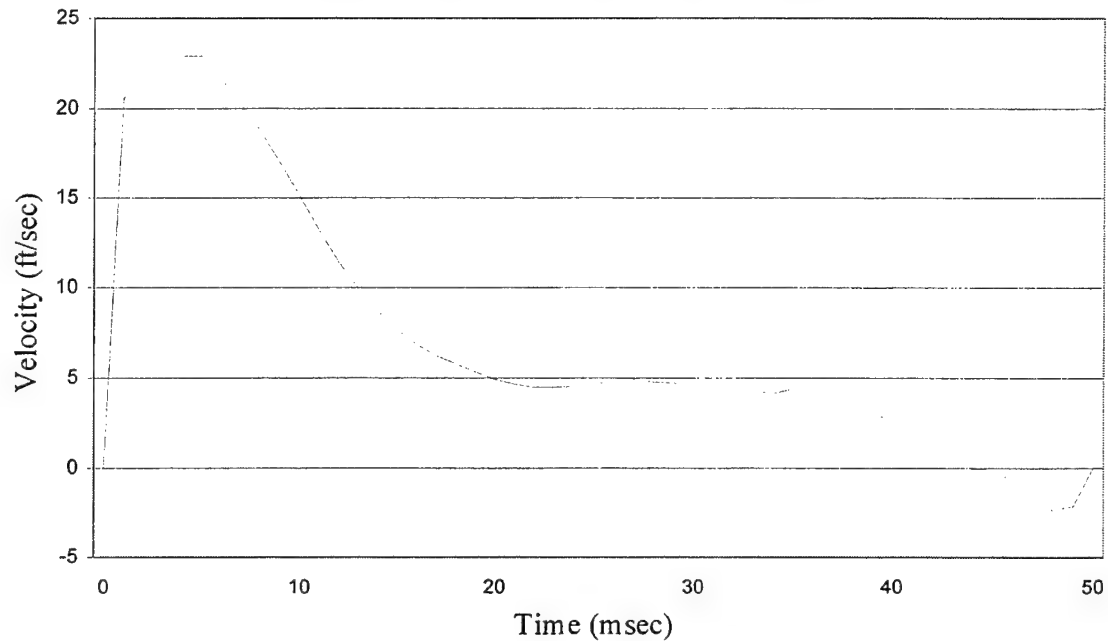
Figure 26: Vertical Response of Barge Model

Node 25 - Coordinate (0,0,12) -Vertical Velocity
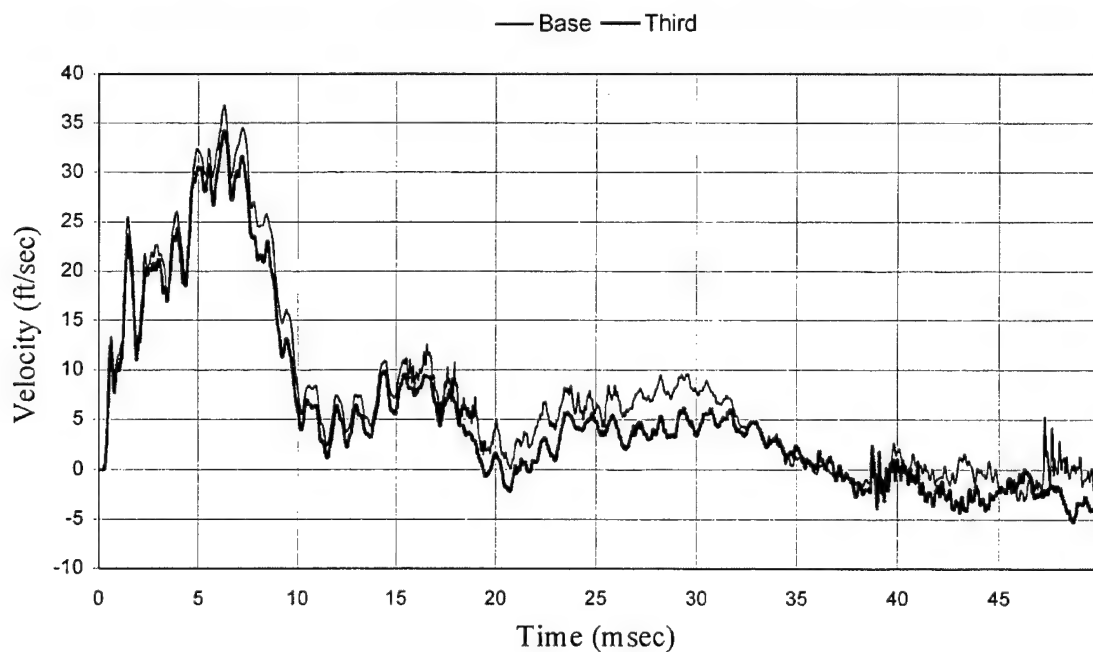
Figure 27: Vertical Response of Node 25 for Base and Half Models

41

The vertical response of node 25 for the Base and Third models are plotted in Figure 27. This node is located at (0,0,12) in the center of the forward bulkhead at the extreme forward end of the barge. Due to its location, the beam bending of the barge structure as well as the plate buckling of the bulkhead influence the vertical response of this node. Initially, the velocity rises sharply due to the impact of the incident shock wave. There is then a sudden drop in the velocity due to the bending response of the structure. This bending response combines with the overall bodily response to cause a high peak velocity of 37 ft/sec. The effect of reducing the fluid volume depth is immediately apparent at approximately 12-msec. At this time the Third model separates from the Base response curve. As Table 4 shows, the phase, magnitude and comprehensive error factors all compare very well for all models analyzed except the Third model. The response is out of tolerance for the Third model based on the Geers magnitude and comprehensive error factors.

Table 4: Russel's and Geer's Error Factor for Node 25

	Extended	Full	Half	Third
Russel				
RM	-0.008	0.004	0.016	0.09
RP	0.068	0.041	0.047	0.06
RC	0.061	0.037	0.044	0.09
Modified Geers				
GM	-0.009	0.005	0.019	0.12
GP	0.023	0.008	0.011	0.02
GC	0.025	0.010	0.022	0.12

The vertical response of node 159 is plotted in Figure 28. This node is located at (50,0,12) in the center of the forward athwartships bulkhead. Table 5 presents the error factors for this node. Both Russel and Geers error factors are above tolerance at this node.

Table 5: Russel's and Geer's Error Factor for Node 159

	Extended	Full	Half	Third
Russel				
RM	-0.005	0.004	0.013	0.10
RP	0.041	0.028	0.037	0.06
RC	0.037	0.025	0.035	0.10
Modified Geers				
GM	-0.006	0.005	0.016	0.13
GP	0.008	0.004	0.007	0.02
GC	0.010	0.006	0.017	0.13

Node 159 - Coordinate (50,0,12) - Vertical Velocity

—— Base —— Third
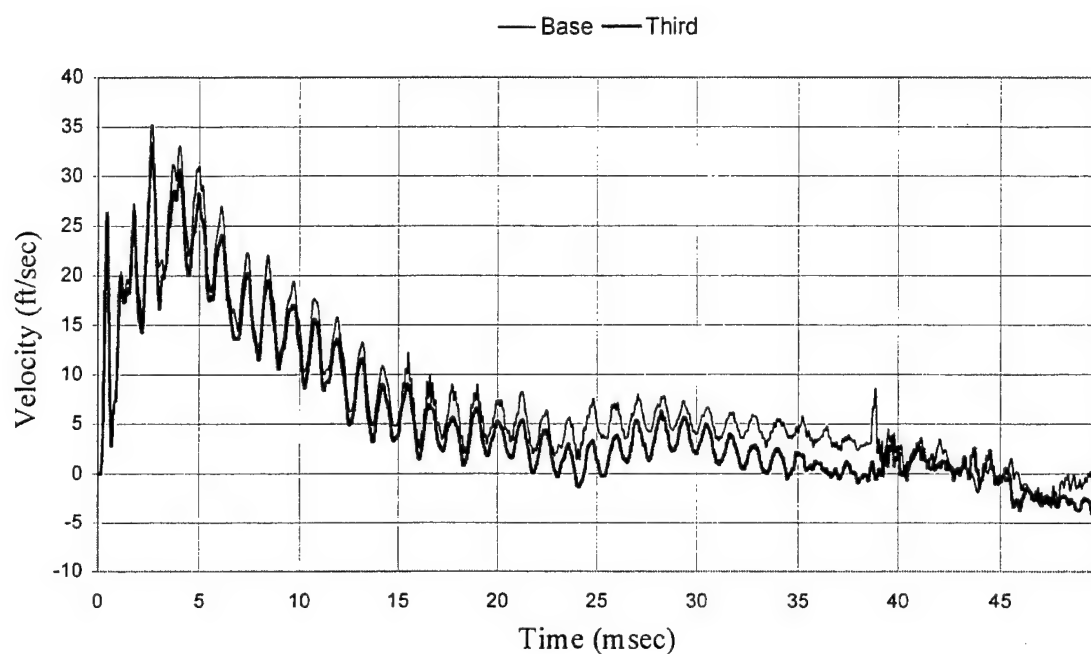
Figure 28: Vertical Response of Node 159 for Base and Half Models

43

Node 285 - Coordinate (118,12,12) - Vertical Velocity

—— Base —— Third
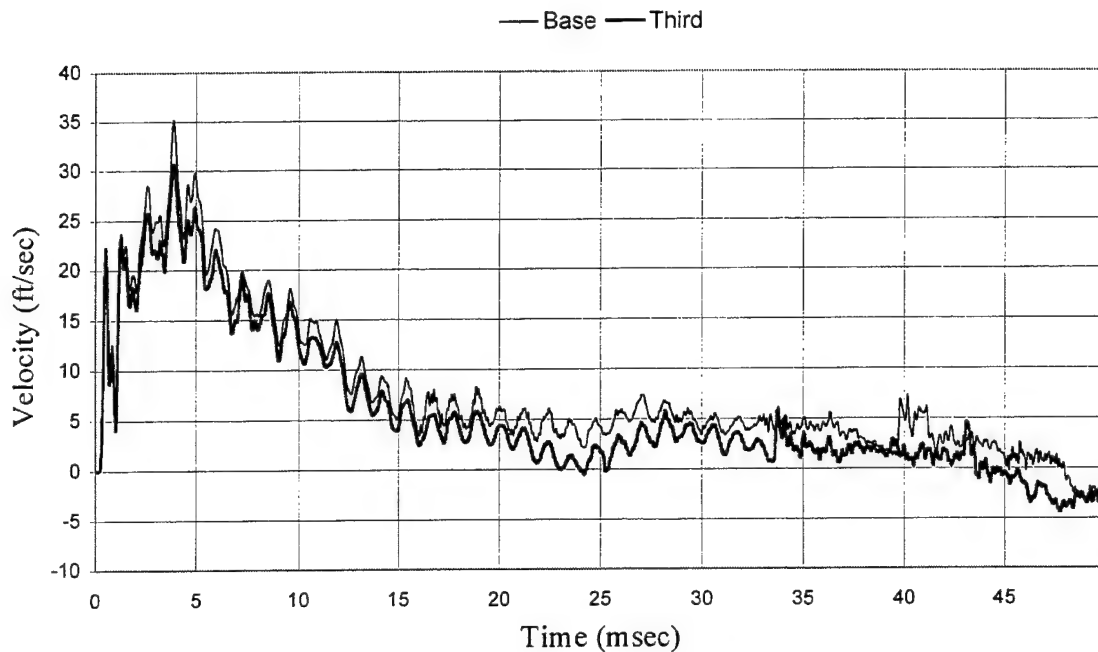
Figure 29: Vertical Response of node 285 for Base and Half Models

The vertical response of node 285 is plotted in Figure 29 and the results of the error analysis in Table 6. This node is located at (118,12,12), on the starboard side of the barge at the intersection of the aft athwartships and side bulkheads. Due to its location, this node is not as affected by the bending response of the barge structure as node 25. Additionally, the stiffness of the location prevents excessive buckling. The response follows that of the overall bodily response, Figure 8, with a high frequency addition. The overall frequency response of the models compares well throughout the run.

Table 6: Russel's and Geer's Error Factor for Node 285

	Extended	Full	Half	Third
Russel				
RM	0.006	0.012	0.022	0.10
RP	0.033	0.037	0.039	0.06
RC	0.030	0.035	0.039	0.10
Modified Geers				
GM	0.007	0.015	0.026	0.14
GP	0.006	0.007	0.007	0.02
GC	0.009	0.016	0.027	0.14

44

The vertical response of node 213 is plotted in Figure 30. This node is located at (84,0,0), on the centerline of the barge in the middle of the floor. This node is located at very flexible point in the structure and at the location of a lumped mass. These two factors damped the response of the structure at this node. The high frequency responses observed in the previous nodes are absent here due to increased flexibility at this location. The negative sign on the magnitude error factors indicate that the magnitude of these models was greater then that of the Base model.

Table 7: Russel's and Geer's Error Factor for Node 213

	Extended	Full	Half	Third
Russel				
RM	-0.008	-0.008	0.003	0.06
RP	0.035	0.020	0.039	0.06
RC	0.032	0.019	0.034	0.08
Modified Geers				
GM	-0.010	-0.009	0.003	0.08
GP	0.006	0.002	0.007	0.02
GC	0.011	0.009	0.008	0.08

Node 213 - Coordinate(84,0,0) - Vertical Velocity

—— Base —— Third
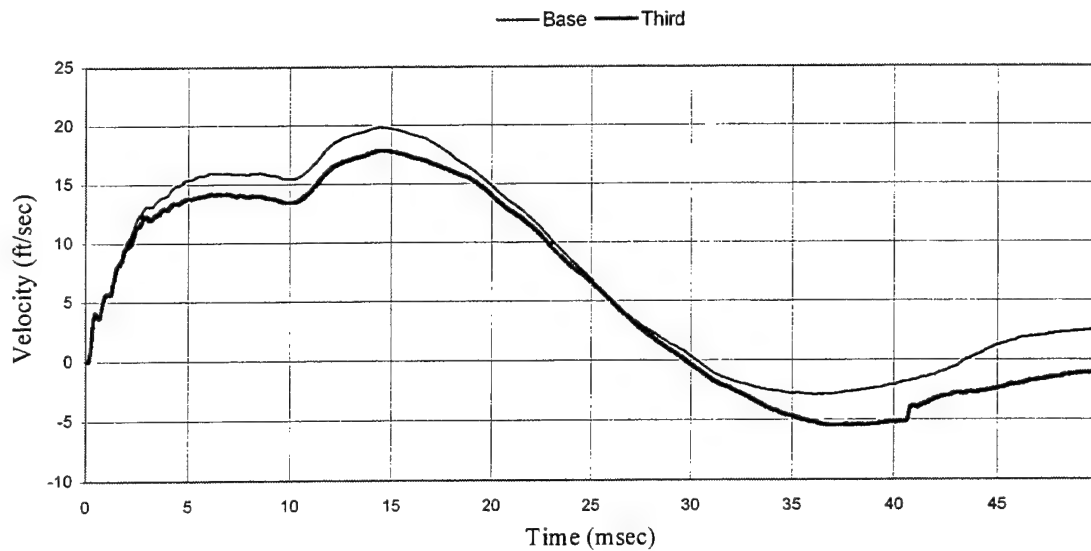
Figure 30: Vertical response of Node 213 for Base and Half Models

Figure 31 shows the vertical response of node 398. This node is located at (142,12,12) on the starboard side bulkhead. This node is located at a very flexible point in the structure and is subjected to plate buckling. Again, the velocity rises sharply and then drops off due to the bending response of the structure. As seen in table 8 the error factors are well under the designated criteria.

Table 8: Russel's and Geer's Error Factor for Node 398

	Extended	Full	Half	Third
Russel				
RM	0.011	0.014	0.025	0.094
RP	0.038	0.043	0.044	0.065
RC	0.035	0.040	0.045	0.101
Modified Geers				
GM	0.013	0.016	0.031	0.128
GP	0.007	0.009	0.009	0.021
GC	0.015	0.019	0.032	0.130

46

Node 398 - Coordinate (148,12,12) - Vertical Velocity
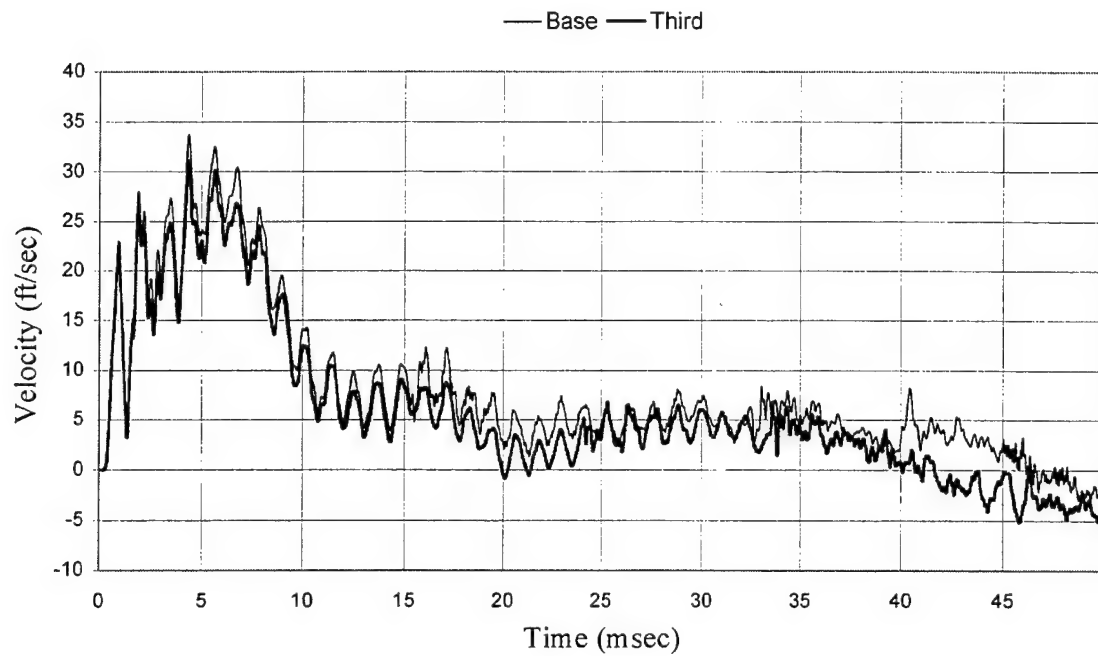
Figure 31: Vertical Response of node 398 for Base and Half Models

C. ATHWARTSHIPS AND LONGITUDINAL RESPONSE

The major excitation on the barge model due to the geometry of this UNDEX attack is vertical. For completeness the longitudinal and athwartships velocity response of several nodes is included. It should be noted that the maximum velocity in these directions is less then 20% of the vertical.

The longitudinal response of node 285 is plotted in Figure 32 and the results of the error analysis in Table 9. This node is located at (118,12,12), on the starboard side of the barge at the intersection of the aft athwartships and side bulkheads. The stiffness of the location prevents excessive buckling. As seen in figure 32 there is poor magnitude and phase correlation between the Base and Third models. Tables 9 and 10 show there is no correlation between all the models for the longitudinal response.

Node 285 (84,0,0) Longitudinal Velocity

— Base ——Third
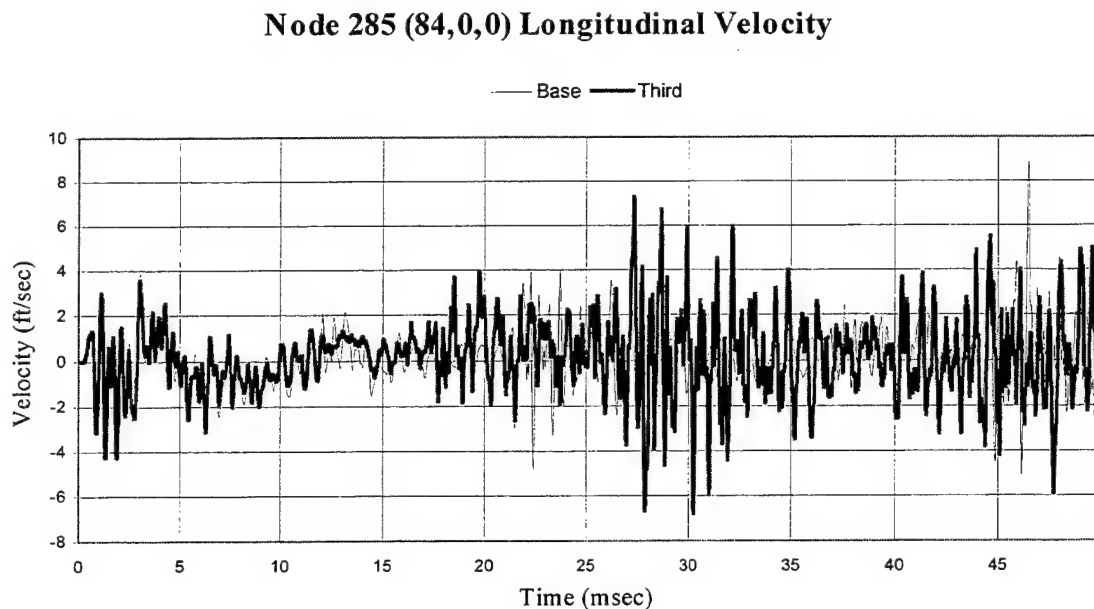
Figure 32: Longitudinal Response of node 285 for Base and Half Models

Table 9: Node 285 Longitudinal Velocity

	Extended	Full	Half	Third
Russel				
RM	-0.060	-0.006	-0.057	-0.203
RP	0.451	0.377	0.435	0.409
RC	0.403	0.334	0.388	0.404
Modified Geers				
GM	-0.072	-0.007	-0.068	-0.255
GP	0.846	0.623	0.796	0.717
GC	0.849	0.623	0.799	0.761

Table 10: Node 213 Longitudinal Velocity

	Extended	Full	Half	Third
Russel				
RM	-0.482	-0.464	-0.141	-0.403
RP	0.451	0.374	0.398	0.432
RC	0.585	0.528	0.374	0.524
Modified Geers				
GM	-0.591	-0.572	-0.174	-0.506
GP	0.848	0.615	0.685	0.788
GC	1.034	0.840	0.706	0.937

Figure 33 shows the athwartships velocity response of node 285. The Base and Third models separate at approximately 15-msec. There is little magnitude and phase correlation between these models. As shown in Tables 11 and 12 all the models experience large errors for the magnitude, phase and comprehensive error factors.

49

Node 285 (84,0,0) Athwartships Velocity

—— Base ——Third
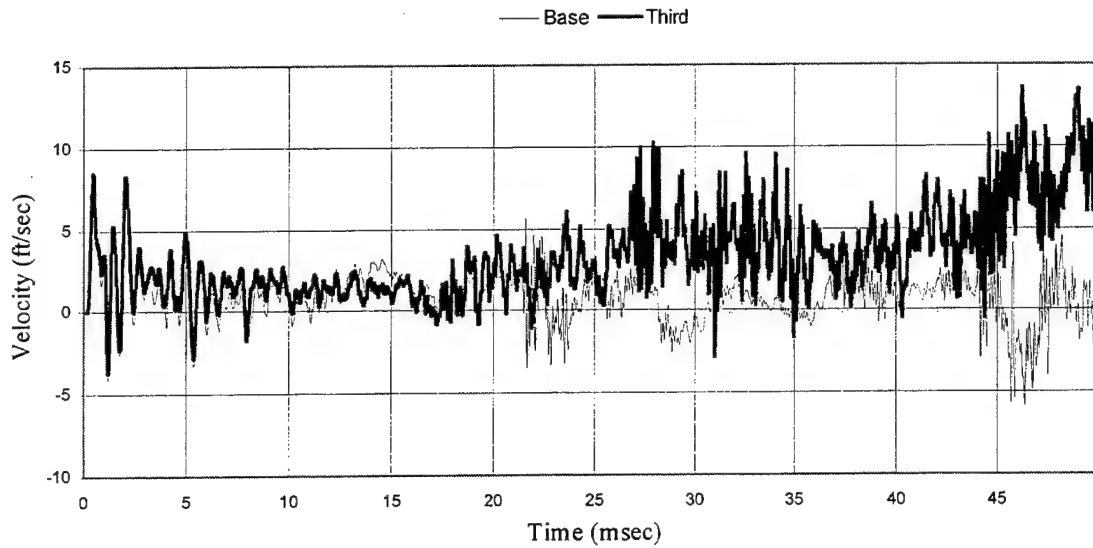
Figure 33: Longitudinal Response of node 285 for Base and Half Models

Table 11: Node 285 Athwartships Velocity

	Extended	Full	Half	Third
Russel				
RM	-0.174	-0.315	-0.537	-0.463
RP	0.295	0.330	0.416	0.395
RC	0.303	0.405	0.602	0.540
Modified Geers				
GM	-0.217	-0.400	-0.643	-0.572
GP	0.398	0.492	0.738	0.677
GC	0.454	0.634	0.979	0.886

Table 12: Node 213 Athwartships Velocity

	Extended	Full	Half	Third
Russel				
RM	-0.110	-0.371	-0.511	-0.618
RP	0.266	0.209	0.351	0.271
RC	0.255	0.378	0.549	0.598
Modified Geers				
GM	-0.134	-0.469	-0.619	-0.709
GP	0.329	0.207	0.549	0.342
GC	0.355	0.513	0.827	0.787

50

VI. CONCLUSIONS AND RECOMMENDATIONS

This thesis reviewed some of the past work done at NPS in surface ship UNDEX modeling and simulation and demonstrated the application of updated software to these problems. The significant advances in computer codes have greatly simplified the task of modeling and simulation. Additionally, this study examined the effect of decreasing the fluid mesh depth on the nodal response of a simple barge structure subjected to an underwater explosion. The time history responses of selected nodes are presented. The Russel and updated Geers error measure criteria are used to quantify the affect of truncating the fluid volume depth. For the vertical response, the Third model was above the 0.1 tolerance for all of the nodes analyzed except node 213. In all cases, the Extended, Full and Half models had error factors of the same magnitude while the Third model was significantly larger. The largest difference in the Russel and Geers error factors are seen in the phase response. This is attributed to the fact that the Russel phase error factor is more sensitive to changes in small and large differences in phasing, and less sensitive in the middle range, compared to the Geers phase error factor [Ref. 19]. The longitudinal and athwartships velocity responses showed little or no correlation between the models. However, since the primary excitation in an UNDEX event is vertical this does not significantly affect the validity of this simulation method. The simulations conducted in this study demonstrate that the fluid mesh may be modeled to approximately one-half of the theoretical cavitation depth and still provide an acceptable vertical response simulation.

Recommendations for areas of additional study:

1.   Work on capturing the full gravitational effects on the barge later in the response. It is suggested that a pressure load can be applied to the structure to more accurately simulate the effect of gravity.

2.   Work is needed to more accurately capture the longitudinal and athwartships response of the structure. Further refinement of the structural finite element model may help in this area.

51

3.   Much consideration is being given in the Navy to advanced hull forms. Utilize this technique to compare the response of various hull forms to the incident UNDEX shock wave. Such hull forms as SLICE, wave-piercing catamaran, and SWATH could be compared to a traditional displacement hull.

APPENDIX A. BULK CAVITATION PROGRAM

The following program code calculates the bulk cavitation zone by solving Equations (2.21) and (2.22).

```
%LT Philip E. Malone


%Bulk cavitation program
clear
Pa = 14.7;
C = 5000;
format short g
disp('1 = HBX-1, 2 = TNT, 3 = Pentolite')
disp('  ')
explosive = input('    Input the number corresponding to the type of
explosive: ');
disp('  ')
weight = input('   Input charge weight(lbs): ');
disp('  ')
D = input ('    Input charge depth(ft): ');
disp('  ')
R = input ('    Input standoff distance in feet: ');
disp('  ')
disp('  ')

% Explosive Paramenters

disp('  ')
W=weight;
if explosive == 1
   K1=22347.6; A1=1.144;
   K2=.056; A2=-.247;
   K3=1.786; A3=.856;
   K4=3086.5; A4=2.039;
   K5=4.761;
   K6=14.14;
elseif explosive == 2
   K1=22505; A1=1.18;
   K2=.058; A2=-.185;
   K3=1.798; A3=.98;
   K4=3034.9; A4=2.155;
   K5=4.268;
   K6=12.67;
else explosive == 3
   K1=24589; A1=1.194;
   K2=.052; A2=-.257;
   K3=1.674; A3=.903;
   K4=3135.2; A4=2.094;
   K5=4.339;
   K6=12.88;
end
```

```
gamma = 0.037037;

%theta = decay constant
%x = horizontal distance
%y = vertical distance
%r1,R = standoff distance from charge to point
%r2 = standoff distance from image charge to point
%Pi = incident shock wave pressure at tc

upper = []; %Create matrix to store upper boundary data
lower = []; %Create matrix to store lower boundary data

%Calculate Upper Boundary
for x = 0:1800
      for y = 0:0.2:200
             r1 = sqrt((D-y)^2+x^2);
             r2 = sqrt((D+y)^2+x^2);
             theta = K2*W^(1/3)*(W^(1/3)/r1)^A2/1000;
      F =(K1*(W^(1/3)/r1)^A1*exp(-(r2-r1)/(C*theta)))+Pa+(gamma*y*12)...
         -(K1*(W^(1/3)/r2)^A1);

             if F <= 0 %Test for cavitation
                   upper = [upper; x y];
             break,end
      end
end

%Calculate lower boundary
for x = 0:(upper(length(upper),1))
      for y = 0:0.2:60
             r1 = sqrt((D-y)^2+x^2);
             r2 = sqrt((D+y)^2+x^2);
             theta = K2*W^(1/3)*(W^(1/3)/r1)^A2/1000;
             Pi = K1*(W^(1/3)/r1)^A1*exp(-(r2-r1)/(C*theta));
      G = -(Pi/(C*theta))*(1+(((r2-(2*D*(D+y)/r2))/r1)*(((A2*r2)/r1)-A2-
1)))...
          -((A1*Pi)/r1^2)*(r2-2*D*((D+y)/r2))+(gamma*12)*((D+y)/r2)+...
          (A1/r2)*(Pi+Pa+(gamma*y*12));

             if G >= 0 %Test for cavitation
                   lower = [lower; x y];
             break,end
      end
end

%Find tangent point
tanu = find(upper(:,2)<lower(:,2));
upper=upper((1:length(tanu)),:);
lower=lower((1:length(tanu)),:);

%Plot cavitation boundary
figure(1)
max_x=max(upper(:,1));
max_y=max(lower(:,2));
maxx=num2str(max_x);
```

```
maxy=num2str(max_y);
wt = num2str(W);
depth = num2str(D);
plot(upper(:,1),-upper(:,2),lower(:,1),-lower(:,2));grid
axis([0,1200,-100,0]);
type=explosive;
if type ==1
title(['Cavitation Zone for a ',wt,' lb HBX-1 Charge at a Depth of
',depth,' feet']);
elseif type==2
   title(['Cavitation Zone for a ',wt,' lb TNT Charge at a Depth of
',depth,' feet']);
else
   title(['Cavitation Zone for a ',wt,' lb Pentolite Charge at a Depth of
',depth,' feet']);
end

xlabel(['feet; where max cavitation width is= ',maxx,' ft'])
ylabel(['feet; where max cavitation depth is= ',maxy,' ft'])
w=W;


%Shock Wave equations
w=W;
r1 = sqrt((D-y)^2+x^2);
r2 = sqrt((D+y)^2+x^2);

theta = K2*W^(1/3)*(W^(1/3)/R)^A2;
Pmax = K1*(W^(1/3)/R)^A1;

I = K3*w^.333*(w^.333/R)^A3; %psi-sec/in^2

E = K4*w^.333*(w^.333/R)^A4; %lb-in/in^3

T = K5*w^.333/(D+33)^(5/6); %sec

Amax = K6*w^.333/(D+33)^.333; %ft
```

55

THIS PAGE INTENTIONALLY LEFT BLANK

This section of this appendix provides example LS-DYNA and USA input decks for each of the three types of models presented: 1D, 2D and 3D. Reference 18 provides information concerning the various input deck variables. The 1D LS-DYNA input is shown first and is completely annotated with the input card descriptions. Use this as a reference when reviewing the other input decks.

1D LS-DYNA input deck

```
$ This input deck contains a complete description of the input cards
$ which are used in the LS-DYNA/USA UNDEX simulations of this study.
$ Reference this deck as you review the input deck for the other models.
$
*KEYWORD
*TITLE
One_D model
$Stops job (time)
*CONTROL_TERMINATION
0.015,0,0,0,0
$Sets structural time step size
*CONTROL_TIMESTEP
$Initial time step size,0,0,0,load curve ID that limits max time step,0
1.0E-6,0.9,0,0.0,0.0,1,0
$Control parrallel processing
*CONTROL_PARALLEL
2,0,1
$Define load curve to limit max timestep
*DEFINE_CURVE
1
0.,1.0E-5
0.015,1.0E-5
$Defines nodes to be stored in NODEOUT file
*DATABASE_HISTORY_NODE
1,2,3,4
$Defines how often NODEOUT file is written to.
*DATABASE_NODOUT
0.00001
$Defines how often D3PLOT file is written to.
*DATABASE_BINARY_D3PLOT
0.00001
$Defines how often D3THDT file is written to.
*DATABASE_BINARY_D3THDT
0.0003
$Defines what data is written to Binary databases.
*DATABASE_EXTENT_BINARY
0,0,3,1,1,1,1,1
0,0,0,0,0,0
$Defines a surface for coupling with USA code.
*BOUNDARY_USA_SURFACE
```

```
$Segment ID, Wet surface flag, SOR
1,1,0
$Defines explosion properties
*INITIAL_DETONATION
$Acoustic boundary, coordinate location of detonation, detonation time...
$Peak pressure at ref node, decay constant, coordinate location
$of ref node, ref node ID
-1,-9540.0,0.0,0.0,0.0
103.0,0.0009968,-1.50,0.0,0.0,5
$
$ NODES
$
*NODE
1,0.000000000E+00,0.000000000E+00,0.000000000E+00,5,7
2,0.000000000E+00,0.000000000E+00,1.50.............
.........
.........
403,-150.000000,1.50000000,1.50000000,0,0
404,-150.000000,0.000000000E+00,1.50000000,0,0
*PART
Fluid (acoustic)
$Part ID, Section ID, Mat'l ID
90,90,90
*SECTION_SOLID
$Defines properties of brick elements
90,8
$Defines properties of acoustic elements
*MAT_ACOUSTIC
$Mat'l ID, mass density, sound speed,damping factor, cavitaion flag...
$atmospheric pressure, gravitational constant
90,9.345E-05,5.712E+04,0.500,1.00,14.7,386.1
$Coordinates of free surface, directional cosine of free surface
0.0,0.0,0.0,1.0,0.0,0.0
$Defines element number, part number, and nodes in element
*ELEMENT_SOLID
1,90,5,6,7,8,1,3,4,2
2,90,9,10,11.....
.........
.........
100,90,401,402,403,404,397,398,399,400
$
$Part one - plate at top of fluid column
*PART
Plate
$Part ID, Section ID, Mat'l ID
1,1,1,0,1,0
$Defines properties of shell elements
*SECTION_SHELL
$Section ID, Element form, Shear factor
1,2,0.8333
$Shell thickness at node
1.0,1.0,1.0,1.0
$Defines element number, part number, and nodes in element.
*ELEMENT_SHELL
1,1,1,3,4,2
```

```
$Defines mat'l properties
*MAT_ELASTIC
$Mat'l ID, Mass density, Youngs modulus, Poisson's ratio
1,5.329E-04,3.000E+07,0.300,,,
$Define the nodes to be constrained.
$Allows x tanslation only.
*BOUNDARY_SPC_SET
1,0,0,1,1,1,1,1
*SET_NODE_LIST
1
1,2,3,4,5,6,7,8
9,10,11,12,13,14,.....
..........
..........
401,402,403,404
$
$Defines a faceset used for DAA boundary
*SET_SEGMENT
1
404,403,402,401,0.000E+00,0.000E+00,0.000E+00,0.000E+00
*END
```

USA input decks for 1D model.

```
FLUMAS DATA FOR 1D Model
flunam geonam strnam daanam          $ FLUNAM GEONAM GRDNAM DAANAM
T T F T                              $ PRTGMT PRTTRN PRTAMF CALCAM
T F F F                              $ EIGMAF TWODIM HAFMOD QUAMOD
F F T F                              $ PCHCDS NASTAM STOMAS STOINV
F F F T                              $ FRWTFL FRWTGE FRWTGR FRESUR
F T F F                              $ RENUMB STOGMT ROTGEO ROTQUA
F F F F                              $ PRTCOE STRMAS SPHERE ROTSYM
F F F F                              $ OCTMOD CAVFLU FRWTFV INTCAV
F F F                                $ BOTREF MASREF BMWHP
0 404 0 1                            $ NSTRC  NSTRF  NGEN   NGENF
0 0 0                                $ NBRA   NCYL   NCAV
9.345E-05 5.712E+04                  $ RHO    CEE
10                                   $ NVEC
0. 1. 0. 0.                          $ DEPTH CXFS CYFS CZFS
14.7 386.088                         $ PATM GRAVAC
0                                    $ NSRADI
0                                    $ NSORDR


AUGMAT DATA FOR 1D MODEL
strnam flunam geonam prenam          $ STRNAM FLUNAM GEONAM PRENAM
F F F F                              $ FRWTGE FRWTST FRWTFL LUMPFM
F T F T                              $ FLUSKY DAAFRM SYMCON DOFTAB
F F F F                              $ PRTGMT PRTTRN PRTSTF PRTAUG
F F F F                              $ MODTRN STRLCL INTWAT CFAPRE
10                                    $ NTYPDA
404 1212 3 3                          $ NSTR   NSFR   NFRE   NFTR
1                                     $ NSETLC
0 1 1 1                          $ NDICOS JSTART JSTOP  JINC
```

```
TIMINT DATA FOR 1D MODEL
prenam posnam            $ PRENAM POSNAM
resnam                   $ RESNAM WRTNAM
F F F F                  $ REFSEC FLUMEM PWACAV ITERAT
F F F                    $ INCSTR CENINT BUOYAN
1 0                      $ NTINT NCHGAL
0.0 1.0E-6               $ STRTIM DELTIM
T F F F                  $ EXPWAV SPLINE VARLIN PACKET
F T F F                  $ HYPERB EXPLOS DOUBDC VELINP
F F F F                  $ BUBPUL SHKBUB
1                        $ NCHARG
0.                       $ HYDPRE
-9540.0,0.0,0.0          $ XC     YC      ZC
-150.0,0.0,0.0           $ SX     SY      SZ
201                      $ JPHIST
1. 0.                    $ PNORM  DETIM
3.0E-5                   $ DTHIST
2                        $ CHGTYP
375.14 795.0 795.0       $ WEIGHT SLANT CHGDEP
2000 2000                $ NSAVER NRESET
0 0 0 0                  $ LOCBEG LOCRES LOCWRT NSTART
F F F F                  $ FORWRT STBDA2 ASCWRT
-1.50,0.0,0.0            $ XV     YV      ZV
F                        $ DISPLA
```

2D model LS-DYNA input deck

```
*KEYWORD
*TITLE
2-D BOX MODEL WITH FLUID 1/Z-AXIS
*CONTROL_TERMINATION
0.1,0,0,0,0
*CONTROL_TIMESTEP
0.00001,0.9,0,0.0,0.0,1,0
*CONTROL_OUTPUT
1,0,1,0,0,1,1
*CONTROL_PARALLEL
2,2,1
*DEFINE_CURVE
1
0.,0.00001
0.10,0.00001
*DATABASE_HISTORY_NODE
1,7,13
*DATABASE_NODOUT
0.00001
*DATABASE_BINARY_D3PLOT
0.0001
*DATABASE_BINARY_D3THDT
0.001
*DATABASE_EXTENT_BINARY
0,0,3,1,1,1,1,1
```

```
0,0,0,0,0,0
*BOUNDARY_USA_SURFACE
2,1,0
*INITIAL_DETONATION
-1,-288.0,-132.0,6.0,0.0
2466.0,0.000321,-4.0,-16.0,6.0,448
$*LOAD_SEGMENT_SET
$2,2,1.,0.0
*NODE
1,0.000000000E+00,-12.0000000,0.000000000E+00,0,0
2,0.000000000E+00,...
.....
.....
627,-108.000000,-40.0000000,0.000000000E+00,0,0
628,-108.000000,-40.0000000,6.00000000,0,0
*PART
solid
        90        2        90
*SECTION_SOLID
          2        8
*ELEMENT_SOLID
1,90,39,40,41,42,1,3,4,2...
....
....
270,90,589,585,588,590,627,623,626,628
*PART
shell
        1        1        1
*SECTION_SHELL
          1        2      0.8333
      0.25      0.25      0.25      0.25
*ELEMENT_SHELL
1,1,1,3,4,2
$
2,1,3,5,6,4
$....
.....
18,1,35,36,38,37
*MAT_ELASTIC
        1   0.000735      3e+07        0.3           0           0           0

*MAT_ACOUSTIC
90,0.9389E-4,59155.2,0.5,1.0,14.7,386.1
12.,0.,0.,1.,0.,0.
*BOUNDARY_SPC_SET
$ This command is used to input a contraint boundary condition on a
$ defined node set.
1,0,0,1,1,1,1,1
*SET_NODE_LIST
1
1,2,3,4,5,6,7,8
.....
.....
625,626,627,628
$ Face set wet
```

61

```
$
*SET_SEGMENT
$ This is the DAA1 boundary.
2
238,237,236,235
.....
.....
589,627,628,590
*END
```

2D USA input decks

Of particular importance in 2D models utilizing the USA code is the numbering of nodes along the DAA1 boundary. This boundary is located around the circumference of the fluid mesh. Imagining the 2D cross-section as a cylinder section, the first two nodes of these DAA1 face elements should progress around the circumference not along the X-Z axis. The NSORDR command in the USA FLUMAS input deck allows the user to cyclically reorder these nodes to achieve this requirement. This my have to be done visually and can be very time intensive.

```
FLUMAS DATA FOR 2D BOX MODEL
flunam geonam strnam daanam        $ FLUNAM GEONAM GRDNAM DAANAM
T T F T                            $ PRTGMT PRTTRN PRTAMF CALCAM
T T F F                            $ EIGMAF TWODIM HAFMOD QUAMOD
F F T F                            $ PCHCDS NASTAM STOMAS STOINV
F F F T                            $ FRWTFL FRWTGE FRWTGR FRESUR
F T F F                            $ RENUMB STOGMT ROTGEO ROTQUA
F F F F                            $ PRTCOE STRMAS SPHERE ROTSYM
F F F F                            $ OCTMOD CAVFLU FRWTFV INTCAV
F F F                              $ BOTREF MASREF BMWHIP
0 628 0 52                         $ NSTRC  NSTRF  NGEN   NGENF
0 0 0                              $ NBRA   NCYL   NCAV
0.9389E-4 59155.2                  $ RHO    CEE
10                                 $ NVEC
12. 1. 0. 0.                       $ DEPTH CXFS CYFS CZFS
14.7 386.088                       $ PATM GRAVAC
0                                  $ NSRADI
19                                 $ NSORDR
0 1 3 1                            $ NORD JBEG JEND JINC
1 4 12 1                           $ NORD JBEG JEND JINC
0 13 14 1                          $ NORD JBEG JEND JINC
1 15 19 1                          $ NORD JBEG JEND JINC
0 20 21 1                          $ NORD JBEG JEND JINC
1 22 23 1                          $ NORD JBEG JEND JINC
0 24 26 1                          $ NORD JBEG JEND JINC
1 27 27 1                          $ NORD JBEG JEND JINC
0 28 29 1                          $ NORD JBEG JEND JINC
1 30 32 1                          $ NORD JBEG JEND JINC
0 33 35 1                          $ NORD JBEG JEND JINC
```

62

```
1 36 37 1                                       $ NORD JBEG JEND JINC
0 38 38 1                                       $ NORD JBEG JEND JINC
1 39 39 1                                       $ NORD JBEG JEND JINC
0 40 43 1                                       $ NORD JBEG JEND JINC
1 44 45 1                                       $ NORD JBEG JEND JINC
0 46 46 1                                       $ NORD JBEG JEND JINC
1 47 47 1                                       $ NORD JBEG JEND JINC
0 48 52 1                                       $ NORD JBEG JEND JINC

AUGMAT DATA FOR 2D BOX MODEL
strnam flunam geonam prenam                     $ STRNAM FLUNAM GEONAM PRENAM
F F F F                                         $ FRWTGE FRWTST FRWTFL LUMPFM
F T F T                                         $ FLUSKY DAAFRM SYMCON DOFTAB
F F F F                                         $ PRTGMT PRTTRN PRTSTF PRTAUG
F F F F                                         $ MODTRN STRLCL INTWAT CFAPRE
11                                              $ NTYPDA
628 1884 3 3                                    $ NSTR   NSFR   NFRE   NFTR
1                                               $ NSETLC
0 1 52 1                                        $ NDICOS JSTART JSTOP  JINC

TIMINT DATA FOR 2D BOX MODEL
prenam posnam           $ PRENAM POSNAM
resnam                  $ RESNAM WRTNAM
F F F F                 $ REFSEC FLUMEM PWACAV ITERAT
F F  F                  $ INCSTR CENINT BUOYAN
1 0                     $ NTINT NCHGAL
0.0 1.0E-5              $ STRTIM DELTIM
T F F F                 $ EXPWAV SPLINE VARLIN PACKET
F T F F                 $ HYPERB EXPLOS DOUBDC VELINP
F F F F                 $ BUBPUL SHKBUB
1                       $ NCHARG
0.                      $ HYDPRE
-288.0,-132.0,6.0       $ XC     YC     ZC
-108.0,-40.0,6.0        $ SX     SY     SZ
201                     $ JPHIST
1. 0.                   $ PNORM  DETIM
6.4E-6                  $ DTHIST
2                       $ CHGTYP
60. 26.0 25.0           $ WEIGHT SLANT CHGDEP
2000 2000               $ NSAVER NRESET
0 0 0 0                 $ LOCBEG LOCRES LOCWRT NSTART
F F F F                 $ FORWRT STBDA2 ASCWRT
-4.0,-16.0,6.0          $ XV     YV     ZV
F                       $ DISPLA
```

3D LS-DYNA input deck

```
*KEYWORD
*TITLE
 BARGE W/OUT BEAMS
*CONTROL_TERMINATION
0.05,0,0,0,0
*CONTROL_TIMESTEP
```

63

```
1.0E-5,0.9,0,0.0,0.0,1,0
*CONTROL_PARALLEL
2,0,1
*DEFINE_CURVE
1
0.,1.0E-5
0.05,1.0E-5
*DATABASE_HISTORY_NODE
213,78,356,303,96
25,159,398,285,267
*DATABASE_NODOUT
0.00001
*DATABASE_HISTORY_SOLID
2257,4279,16077,18257
2239,7413,6322,6327
6333,6339,6342
*DATABASE_ELOUT
0.00001
*DATABASE_BINARY_D3PLOT
0.001
*DATABASE_BINARY_D3THDT
0.003
*DATABASE_EXTENT_BINARY
0,0,3,1,1,1,1,1
0,0,0,0,0,0
*BOUNDARY_USA_SURFACE
1,1,0
*INITIAL_DETONATION
-1,84.0,-132.0,-288.0,0.0
2466.0,0.000321,84.0,-16.699,-4.0,3757
$
*NODE
1,0.000000000E+00,-12.0000000,0.000000000E+00,0,0
23277,84.0000000,-64.0000000,-300.000000,0,0
*PART
Fluid (acoustic)
90,4,90
*SECTION_SOLID
4,8
*ELEMENT_SOLID
1,90,444,445,446,447,1,8,9,2
.....
.....
20592,90,22489,22171,22174,22491,23266,22948,22951,23268
*PART
Shell Plating
3,3,1
*SECTION_SHELL
3,2,0.8333
0.25,0.25,0.25,0.25
*ELEMENT_SHELL
1,3,1,8,9,2
$
2,3,8
```

```
$
$ Face set wet
$
*SET_SEGMENT
1
699,698,697,696,0.000E+00,0.000E+00,0.000E+00,0.000E+00
.....
.....
7715,7720,8497,8492,0.000E+00,0.000E+00,0.000E+00,0.000E+00
*MAT_ELASTIC
1,7.350E-04,3.000E+07,0.300
$
*MAT_ACOUSTIC
90,9.345E-05,5.916E+04,0.5,1.0,14.7,386.088
0.,0.,12.0,0.,0.,1.00
*ELEMENT_MASS
1,69,0.664
2,213,0.664
3,350,0.664
*END
```

3D USA input decks

```
FLUMAS DATA FOR 3D BOX MODEL
flunam geonam strnam daanam        $ FLUNAM GEONAM GRDNAM DAANAM
F F F T                            $ PRTGMT PRTTRN PRTAMF CALCAM
T F F F                            $ EIGMAF TWODIM HAFMOD QUAMOD
F F T F                            $ PCHCDS NASTAM STOMAS STOINV
F F F T                            $ FRWTFL FRWTGE FRWTGR FRESUR
F T F F                            $ RENUMB STOGMT ROTGEO ROTQUA
F F F F                            $ PRTCOE STRMAS SPHERE ROTSYM
F F F F                            $ OCTMOD CAVFLU FRWTFV INTCAV
F F F                              $ BOTREF MASREF
0 23277 0 3968                     $ NSTRC  NSTRF  NGEN   NGENF
0 0 0                              $ NBRA   NCYL   NCAV
0.9345E-4 59160.0                  $ RHO    CEE
5                                  $ NVEC
12. 0. 0. 1.                       $ DEPTH CXFS CYFS CZFS
14.7 386.088                       $ PATM GRAVAC
0                                  $ NSRADI
0                                  $ NSORDR

AUGMAT DATA FOR 3D BOX MODEL
strnam flunam geonam prenam        $ STRNAM FLUNAM GEONAM PRENAM
F F F F                            $ FRWTGE FRWTST FRWTFL LUMPFM
F T F T                            $ FLUSKY DAAFRM SYMCON DOFTAB
F F F F                            $ PRTGMT PRTTRN PRTSTF PRTAUG
F F F F                            $ MODTRN STRLCL INTWAT CFAPRE
11                                 $ NTYPDA
23277 69831 3 3                    $ NSTR   NSFR   NFRE   NFTR
1                                  $ NSETLC
0 1 3968 1                         $ NDICOS JSTART JSTOP  JINC
```

65

```
TIMINT DATA FOR 3D BOX MODEL
prenam posnam            $ PRENAM POSNAM
resnam                   $ RESNAM WRTNAM
F F F F                  $ REFSEC FLUMEM PWACAV ITERAT
F F F                    $ INCSTR CENINT BUOYAN
1 0                      $ NTINT NCHGAL
0.0 1.0E-5               $ STRTIM DELTIM
T F F F                  $ EXPWAV SPLINE VARLIN PACKET
F T F F                  $ HYPERB EXPLOS DOUBDC VELINP
F F F F                  $ BUBPUL SHKBUB
1                        $ NCHARG
0.                       $ HYDPRE
84.0,-132.0,-288.0       $ XC      YC      ZC
84.0,-64.0,-300.0        $ SX      SY      SZ
201                      $ JPHIST
1. 0.                    $ PNORM   DETIM
6.4E-6                   $ DTHIST
2                        $ CHGTYP
60. 26.0 25.0            $ WEIGHT SLANT CHGDEP
2000 2000                $ NSAVER NRESET
0 0 0 0                  $ LOCBEG LOCRES LOCWRT NSTART
F F F F                  $ FORWRT STBDA2 ASCWRT
84.0,-16.6699,-4.0       $ XV      YV      ZV
F                        $ DISPLA
```

APPENDIX C. FLUID MODELING USING TRUEGRID

This appendix covers the procedure for creating a fluid finite element mesh using TrueGrid. Some of these techniques were adopted from Reference 17. Two of the most useful features of TrueGrid for coupled fluid modeling are the **BLUDE** and **BB** commands. The basics of using TrueGrid will not be covered here and some familiarity with the code is assumed. An example of a partial batch file is included. This batch file creates a basic barge and extrudes a fluid mesh. Additional information can be found in the TrueGrid user manual. [Ref. 8]

The **BLUDE** command "extrudes" the structural mesh through a user defined grid or block of mesh mated to the structural wetted surface. The block part is actually attached to a surface definition created from a faceset of the wetted elements of the structural mesh. The resulting extruded mesh matches exactly to the structural mesh, a prerequisite for successful fluid modeling.

The extrusion procedure is as follows, with important commands and menu selections denoted in bold and all capital letters for emphasis:

1. A structural model must be created. TrueGrid can be used or the **READMESH** command can be used to input a mesh from another code format. It is very important to remember though, that when TrueGrid reads in a finite element mesh from an outside code format, it renumbers every element and grid point. Therefore, once the mesh is through being manipulated in TrueGrid, and it is written an output file, the grid point and element ID numbers will not match between the original and newly output model from TrueGrid.

2. The elements of the structural model that will be in contact with the fluid, i.e. the wetted surface, must be grouped into **FACESETS**. This option can be accessed from the environment window under the **PICK** option by choosing the **SETS** button. The **FACES** button should be selected. Appropriate faces of the models wet surface should be put in a separate **FACESET**. Pick faces which are naturally defined by the geometry of the wet surface. For a rectangular barge this includes the bottom, sides, bow and stern below the waterline. For a ships hull this would include the port and starboard sides and the stern. In this case the bow is typically a

sharp edge and would not be selected as a **FACESET**. The **HIDE** drawing mode vice **WIREFRAME** should be used for the mesh to ensure that only the visible elements are picked. This will make faceset selection must easier, since it must be done by hand using the lasso tool guided by the mouse. The three- or four-node selection option is the best to use when choosing the faceset. This means that three or four nodes of an element must be within the selection lasso for the element to be added to the faceset. The selected elements will be highlight in white. If some elements are selected that are not desired in the particular set, they can be easily selected and removed; using the one node selection option is best for this operation. The **REMOVE** button should be pushed also. The set must be named and saved once selected.

3. The **SURFACE** menu **SD** (surface definition) option should be chosen next. A surface number must be input. The faceset option should be selected from the end of the surface options list and the name of the desired faceset should then be input. This step converts the named faceset into a surface definition. The new surface will be displayed in red in the physical window. This is also useful in troubleshooting the faceset. The **SURFACE** created should have no holes in it. These holes would represent elements that were missed in the **FACESET** selection.

4. Next, the **PARTS** menu should be selected and the **BLUDE** option chosen. Using this option, the user creates a block part that will be attached to the surface created above. This block will serve as the "guide" for the extrusion of the structural mesh; therefore, the block's mesh must match the structural mesh or be of finer quality in order to get a quality extrusion; an exact match is not required however. This block part is created in the same way as a block using the **BLOCK** command. The blude command requires two additional inputs, however. First, the name of the face of the block where the extrusion begins must be input. This is simply the face closest to the structure. Next, the name of the faceset to be extruded must input.

5. The block part created can now be manipulated to obtain the desired geometry. This is the "art" behind TrueGrid and requires practice to be done successfully. The part created must now be attached to the surface defined in step 3. It can be attached

68

using any of TrueGrid's available options. The **PROJECT** button in the environment window is the easiest to use. This will work for simple cases, but a complex surface may require use of other TrueGrid methods.

6. The interface of the extrusion mesh and the structural mesh should be carefully examined. Orthogonality of the fluid and structural mesh is a must (next to the wetted surface) and should be verified; TrueGrid's **DIAGNOSTICS** menu provides the necessary tools. The block mesh can be modified as needed using various TrueGrid tools to ensure a quality mesh is constructed for the extrusion; two examples of useful tools are the mesh relaxation algorithms and use of a cubic spline to added curvature to the block mesh edges. Material properties can be assigned to the mesh also, just as with any other part in TrueGrid.

7. Once the user is satisfied with the mesh, the **MERGE** command should be used to end the **PARTS** phase. The result will be a fluid mesh, which matches exactly to the structural mesh. The mesh will consist of 8-noded solid elements. The **STP** option should be reviewed and used to fully merge all the nodes on the interface of the structure and the extruded mesh. Prior to merging, the extrusion mesh can be replicated using the **LCT** and **LREP** commands. This will only be effective if the model is symmetric. Using these part replication features, the user only has to build one-half of the extrusion mesh.

8. Additional extrusions can be performed, including on any newly extruded mesh surfaces. This must usually be done to fully form a fluid mesh around the structural model.

The BB command defines a block boundary interface for parts that will interact with one another. This command allows the user to save the geometry of a face, edge or vertex of a part and use it to form the geometry of another at a later time. This feature is used in the PART (or BLUDE) phase. The useful features of this command for fluid modeling will be highlighted here.

1. In the PART phase the user selects the face of a part for future reference and gives it a specific name. This is done with the BB command, the region and a name. The

user can select the region in the computational window and print the region with the F1 button. For example BB 1 1 1 5 5 1 12, defines the master side of a block boundary as region 1 1 1 25 5 1 and names it 12.

2. Use ENDPART or MERGE to complete the above part.

3. In the PART phase the user selects the face of the part that must match the MASTER defined above. Use the same technique. Now define the BB command again with the newly selected region and the same block boundary number as the MASTER. For example BB 1 1 2 2 2 2 12, matches the region 1 1 2 2 2 2 to the region 1 1 1 5 5 1.

Example of a TrueGrid batch file to create a coupled barge/fluid model.

Material Definitions use the **mate** command.

```
c mate 3 is structural steel for shells
lsdymats 3 1 struct rho .735e-3 e .300e+08 pr .300 ;
c mate 90 is fluid
lsdymats 90 90 rho .9389e-4 ss 59155.2 b .5 cf 1 fsp 0 0 12 fsn 0 0 1;
```

The **block** command creates the basic barge structure. The negative signs generate shells. The **thic** command defines the shell thickness. The **mate** command assigns a part and material number. This will be the part number used in the LS-DYNA input deck.

```
block -1 -6 -12 -17; -1 4 -7; -1 7;
0 50 118 168; -12 0 12; 0 24;
thic .25 mate 3;
```

```
merge
```

Use the **pick sets** command to pick the bottom faces of the barge. Define this set as a surface with the **sd** command. Do the same for the bow and stern below the waterline.

```
fset bottom = ls
c linear shells
 49:63 82:96 181:198 217:234 319:333 352:366;;
sd 1 faceset bottom

fset fwd = ls
c linear shells
 1:9 64:72;;

fset aft = ls
c linear shells
 397:405 415:423;;

sd 2 faceset fwd
```

70

```
sd 3 faceset aft
```

Use the **blude** command to generate a block of mesh to extrude the faceset on the bow of the barge through. Do the same for the stern. Define the fluid mesh as mate 90. The **res** command is used to vary the mesh density in the fluid volume.

```
blude 2 fwd
1 11; 1 7; 1 4;-84 0; -12 12;0 12;
res 1 1 1 2 2 2 i .86957
mate 90
sfi -2;;;sd 2
merge

blude 1 aft 1 11; 1 7; 1 4;168 252; -12 12;0 12;mate 90
res 1 1 1 2 2 2 i 1.15
sfi -1;;;sd 3
merge
```

The above commands generate two sections of the coupled fluid volume off the bow and stern. Next two facesets are defined along the port and starboard sides of the new coupled barge/fluid model.

```
fset stbd = lb3
c linear bricks - face #3
 51:60 81:90 141:150 241:250 281:290 341:350;
c linear shells
ls 97:111 235:252 367:381;;

sd 4 faceset stbd
fset port = lb5
c linear bricks - face #5
 1:10 21:30 151:160 181:190 201:210 321:330;
c linear shells
ls 19:33 145:162 289:303;;

sd 5 faceset port
```

The fluid is extruded out to the port and starboard with the next commands.

```
blude 4 port 1 60;1 8;1 4;
-84 252;-64 -12;0 12;
mate 90
res 1 1 1 2 2 2 j .86957
sfi ; -2;;sd 5

merge

blude 3 stbd 1 60;1 8;1 4;
-84 252;12 64;0 12;
mate 90
res 1 1 1 2 2 2 j 1.15
sfi ; -1;;sd 4
merge
```

The next command defines a faceset on the bottom of the coupled barge/fluid model. This is then sxtruded to the desired depth.

```
fset bottom = lb2
c linear bricks - face #2
 1:20 41:50 81:90 101:110 131:140 181:200 211:220 281:290 311:320 351:360

 1726:1732 1740:1746 1775:1781 1803:1809 1824:1830 1838:1844 1866:1872;
c linear shells
ls 49:63 82:96 181:198 217:234 319:333 352:366;;

sd 6 faceset bottom

blude 6 bottom 1 31;1 30; 1 21; -84 252; -64 64;-120 0;mate 90
as 1 1 1 2 2 2 k 1 4
sfi ;; -2;sd 6
merge
RP 1
```

Now that the entire fluid volume has be created, a faceset is defined on all of its exposed faces except the free surface. This faceset is the DAA1 boundary. The **orpt** command ensures the nodal numbering of this faceset set generates outward facing normals. This is crucial for proper behavior of the analysis. A good trouble shooting technique is to create a surface of this faceset (**sd 7 faceset wet**) and then remove the mesh with the **rap** command. This surface should no holes in it and on the edge along the free surface should be visible when it is rotated. The **dap** command is used to restore the mesh.

```
orpt - 0 0 0

fset wet = lb1
c linear bricks - face #1
 10 20 30 40 50 60 70 80 90
sd 7 faceset wet
```

The **output** command can now be used to generate an LS-DYNA input deck.

APPENDIX D: SECOND GENERATION DDG53 COUPLED MODEL

This Appendix details the modeling of a second-generation coupled structural-fluid model for the simulation of the shock trial of USS JOHN PAUL JONES (DDG53). Some of the results of a simulation conducted using a first-generation model were presented in Ref. 7. This paper showed promising results in simulating the vertical response of the DDG53 when compared to the ship shock trial data. Further investigation into the coupled structure-fluid model was desired to improve the nodal distribution in the coupled fluid mesh. Specific areas of interest were along the keel line and bow. The extreme geometries of the sonar dome presented a significant problem in the meshing of the model. This model uses the same three-dimensional finite-element model of the USS JOHN PAUL JONES (DDG53) developed by Gibbs and Cox, Inc. [Ref. 22]. Table D1 compares the characteristics of the old and new coupled models.

Table D1: Comparison of Coupled Fluid Models

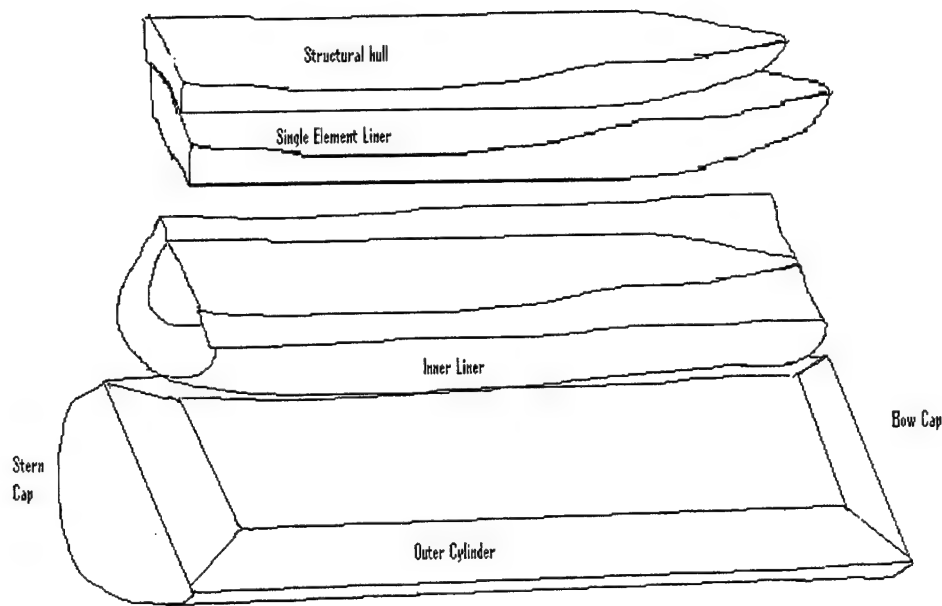| Characteristic	Old Model	New Model
Number of Total Nodes	174,635	198,130
Number of Fluid Nodes	139,664	162,930
Number of Ship Nodes	34,971	35,200
Number of Fluid Elements	94,199	132,810
Number of DAA1 Faces	4,290	5202

Figure D1: Sketch of Modeling Scheme

Figure D1 shows the basic scheme utilized in constructing the fluid volume. This scheme seems very effective in dealing with the complex geometries of a ships hull. It shows the structural hull fitted within a single element thick liner. This liner is used to smooth the discontinuities in the ships wet surface. An inner liner is then extruded from this single element liner to give the fluid volume a cylindrical shape. The inner cylinder is fitted into an outer cylinder that represents the bulk of the fluid volume. Bow and stern caps are then extruded from the inner cylinder to plug the ends of the outer cylinder.

The intent of this Appendix is to provide a near step-by-step approach to constructing a coupled fluid volume to a ships hull. The DDG53 model will be used as an example of the procedure. The courier 10 text is from the actual TrueGrid batch file. It is included here as an example of the command syntax. This is NOT a complete batch input deck. This model was constructed with the assistance of Dr. Robert Rainsberger of XYZ Scientific, Inc. His help was invaluable.

```
c this file loads the ddg nastran deck and deletes the springs

parameters or 1344 c outer radius
bh 1000 c distance behind the stern
smooth 1; c smoothing flag
```

The **readmesh** command reads in a supported codes mesh and converts it to a TrueGrid part. The **endpart** command is used to finish that part definition.

```
readmesh nastran sp_2nf0f.bdf
endpart

merge
```

The **delspds** command deletes the defined numbered springs.

```
delspds 1:416;
```

The **block** command is used here to create a patch of mesh to plug the hole in the ships hull where the propeller shafts extend through.

```
c  fill the shaft hole in the ship
block 1 2 3 4 5 6 7 8;
     -1;
     1 2 3 4;
     1152 1200 1248 1296 1344 1392 1440 1488
     -135
     60 71 82 95
endpart

c  fill the shaft hole in the ship
block 1 2 3 4 5 6 7;
     -1;
     1 2 3 4;
     1152 1200 1248 1296 1344 1392 1440
     135
     60 71 82 9
endpart

merge
```

The **pick sets** option, described in Appendix C, is used here to create two **faceset's** of the wet surface of the ships hull, starbrd and port. This translates to **fset** in the batch file. Two surfaces are then created from these facesets, sd 1 and sd 2.

```
c  create a face set of all of the polygons forming the exterior of the
ship

fset starbrd = ls
fset port = ls

c  form the two surfaces of the wet ship
sd 1 faceset starbrd
sd 2 faceset port

c  extract the edges of the new surfaces as curves
curd 1 se 1.2
curd 2 se 1.3
```

```
curd 3 se 2.1
curd 4 se 2.3
c   create curves that form the special region along the keel
```

The **pick sets** option is used here to create a **faceset** of the bottom of the sonar dome.

```
c   form a face set of the bottom polygons along the sonar dome
fset sonar = ls 1223:1260;;
```

The **blude,** described in Appendix C, command is used here extrude the sonar dome mesh one element orthogonally.

```
c
blude 6 sonar 1 61;1 20 39;1 2;4896 5581 88 0 -88 -9 0;

endpart
```

The **block and bb** commands are used here to generate a block boundary interface. The bb interface will be used to form the single element liner.

```
c   create the starboard block boundary interface part
c   the part is not used, just the block boundary interfaces
block 1 194;-1 2;-1 -24;0 5584 0 0 0 254

 bb 1 1 1 2 1 2 1;
 bb 1 2 1 2 2 1 3;
 bb 1 2 2 2 2 2 5;

 mate 0

endpart
```

The **blude** command is used here to extrude the starboard side mesh one element orthogonally.

```
c   create the first orthogonal layer of elements along the starbooard
blude 4 starbrd 1 194;1 2;1 24;0 5584 -9 0 0 254

 bb 1 2 1 2 2 2 1;
 bb 1 1 1 2 1 2 1 normal 9;
 bb 1 1 1 2 1 1 3;
 bb 1 1 2 2 1 2 5;

endpart
```

The **block and bb** commands are used here to generate a block boundary interface. The bb interface will be used to form the single element liner.

```
c   create the port block boundary interface part
c   the part is not used, just the block boundary interfaces
block 1 194;-1 2;-1 -24;0 5584 0 0 0 254

 bb 1 1 1 2 1 2 2;
 bb 1 2 1 2 2 1 4;
```

```
bb 1 2 2 2 2 2 6;

mate 0

endpart
```

The **blude** command is used here to extrude the port side mesh one element orthogonally.

```
c  create the first orthogonal layer of elements along the port
blude 3 port 1 194;1 2;1 24;0 5584 0 9 0 254

bb 1 1 1 2 1 2 2;
bb 1 2 1 2 2 2 2 normal -9;
bb 1 2 1 2 2 1 4;
bb 1 2 2 2 2 2 6;

endpart

merge
```

The port and starboard liners created above leave a gap along the keel line. The **block** command is used to create a series of wedges to fill in this gap.

```
c  create the wedge elements filling in the gap
block      1    2    3    4    5    6    7    8    9
      10   11   12   13   14   15   16   17   18   19
      20   21   22   23   24   25   26   27   28   29
      30   31   32   33   34   35   36   37   38   39
      40   41   42   43   44   45   46   47   48   49
      50   51   52   53   54   55   56   57   58   59
      60   61   62   63   64   65   66   67   68   69
      70   71   72   73   74   75   76   77   78   79
      80   81   82   83   84   85   86   87   88   89
      90   91   92   93   94   95   96   97   98   99
     100  101  102  103  104  105  106  107  108  109
     110  111  112  113  114  115    0  117  118  119
     120  121  122  123  124  125  126  127  128  129
     130  131  132  133;
       1 2 3 0 5 6 7;
       1 2;
       0 0 0 0 0 0 0 0 0 0 0 0 0 0 0 0 0 0 0 0 0 0 0 0 0 0 0 0 0 0 0
       0 0 0 0 0 0 0 0 0 0 0 0 0 0 0 0 0 0 0 0 0 0 0 0 0 0 0 0 0 0 0
       0 0 0 0 0 0 0 0 0 0 0 0 0 0 0 0 0 0 0 0 0 0 0 0 0 0 0 0 0 0 0
       0 0 0 0 0 0 0 0 0 0 0 0 0 0 0 0 0 0 0 0 0 0 0 0 0 0 0 0 0 0 0
       0 0 0 0 0 0 0 0 0 0 0 0 0 0
       0 0 0 0 0 0 0
       0 0
```

The **dei** command is used to delete elements.

```
dei 1 115;1 2 0 6 7;;

endpart
```

The **sd and cy** commands are used to create two surfaces that will define the inner and outer fluid mesh cylinders (see figure D1).

```
sd 11 cy 0 0 254 1 0 0 529 c intermediate cylinder
sd 26 cy 0 0 254 1 0 0 %or c outer cylinder
```

The **pick sets and sd** options are used to create a surface of the stern.

```
fset stern = lb2

sd 23 faceset stern
block 1 2;1 2 3 4 5;1 2 3 4 5 6 7 8 9 10 11;

endpart
```

The **block** command is used to create a block of mesh on the stern.

```
block 1 2;1 2 3 4 5;1 2 3 4;5.5813301e+03 5.5813301e+03 0 0 0 0 0 0 0 0 0
dei ;1 2 0 4 5;1 2 0 3 4;

merge
```

The **pick sets and sd** options are used to create a surface of the exterior faces of the single element liner. This faceset and surface will be used to extrude the bulk of the coupled fluid volume.

```
c make a face set of the exterior faces of the first orthogonal layer
fset hull = lb1

sd 10 faceset hull
```
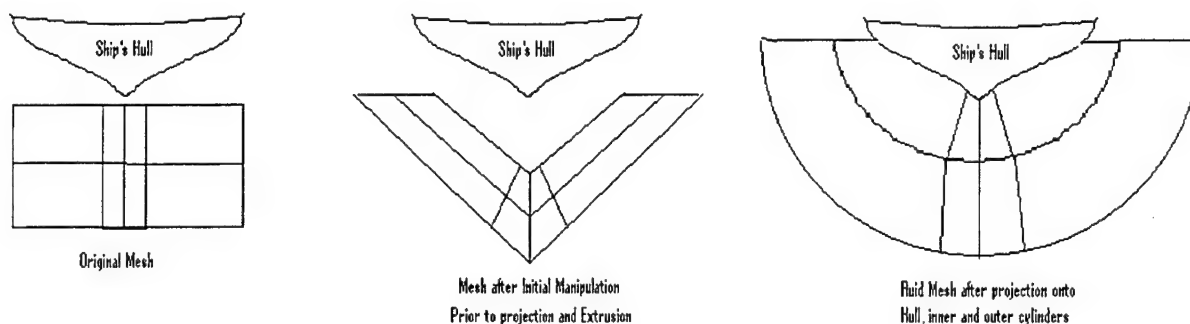
Figure D2: Extrusion of Bulk Fluid

The **blude** command is used to extrude the bulk of the fluid from the faceset defined above, fset hull. This block of mesh is manipulated to form the desired geometry for the extrusion. The mesh is then projected onto the inner and out cylinders defined above. The **bb** command is used here to create a set of master block boundary interfaces to be used for the bow and stern caps. See figure D2.

```
blude 6 hull 1 3 5 7 9 11 13 15 17;
 1 3 5 7 9 11 13;
 1 3 5;
 -1.3062277e+00 8.6497479e+02 9.6269177e+02 1.0584098e+03
 4.2724814e+03 4.9031758e+03 5.1360000e+03 5.4480044e+03
 5.5921299e+03;
 -300 -90 -87 0 87 90 300;
 -900 -408 0;
mseq i 28 2 2 80 22 7 10 8
mseq j 15 0 0 0 0 15
mseq k 8 16

bb 9 1 1 9 4 2 7;
bb 9 4 1 9 7 2 8;
bb 1 4 1 1 7 2 9;
bb 1 1 1 1 4 2 10;

endpart
```

The **pick sets** command is used to select the fantail of the ship model. This set is then extruded to form a block of mesh.

```
fset p_fan = ls
sd 31 faceset p_fan
```

79

```
blude 2 p_fan 1 11;1 17;1 6;
-493.3 0;-228.75 228.75;219.5 304;
sfi -2;;;sd 31
```

The **pick sets** command is used to select the faces of the stern fluid needed to construct the stern cap. The **blude** command is used to extrude the mesh of the inner cylinder to the end of the model. The **bb** command is used to define the slave side of the block boundary interfaces, 9 and 10, defined above. This allows the mesh that is extruded from the inner cylinder to be projected down onto the outer cylinder mesh. The **btol** command is used to merge the nodes between parts 12 and 14. Part 12 is the bulk fluid and part 14 is the stern cap. A similar procedure is used for the bow cap.

```
fset prt_strn = lb2
sd 53 faceset prt_strn
fset stb_strn = lb3
sd 54 faceset stb_strn
fset strn_flu = lb2
sd 35 faceset strn_flu

blude 2 strn_flu 1 11; 1 13 25; 1 22;-493.3 0;-228.75 0 228.75;
-156 219;

bb 1 1 1 2 2 1 10;
bb 1 2 1 2 3 1 9;

merge
RP 1

bptol 13 14 4
bptol 12 14 4
```

The procedure for the bow cap is similar to the stern cap above.

```
fset fwd_plug = lb1
sd 42 faceset fwd_plug

fset fwd_port = lb2
sd 43 faceset fwd_port

fset fwd_stbd = lb3
sd 44 faceset fwd_stbd
blude 1 fwd_plug 1 11;1 22 43;1 21;5604 6084;-254 0 254;-150 0;

bb 1 1 1 2 2 1 7;
bb 1 2 1 2 3 1 8;

bptol 12 15 3
```

The fluid mesh is complete. As detailed in Appendix C, the outward faces of the completed fluid mesh are selected with **pick faces** command. This faceset is the DAA1 boundary for the model.

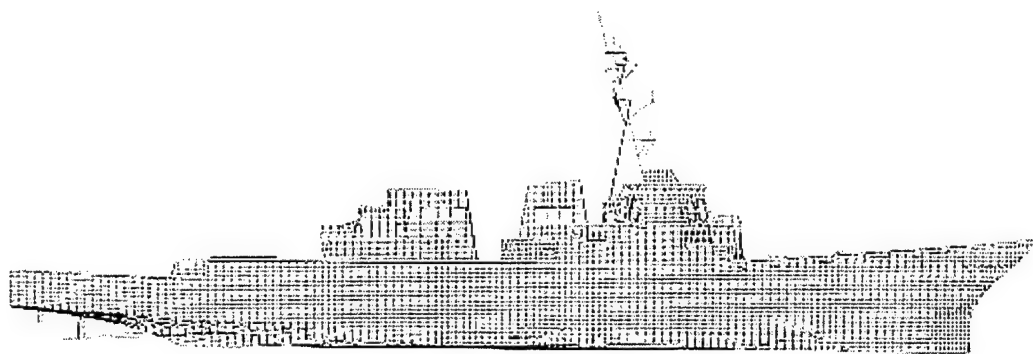The following figures show the details of the modeling of the USS John Paul Jones (DDG53) coupled fluid model.

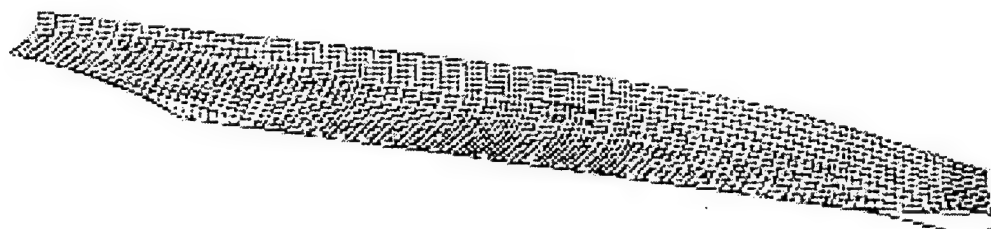

Figure D3: DDG53 Structural Model
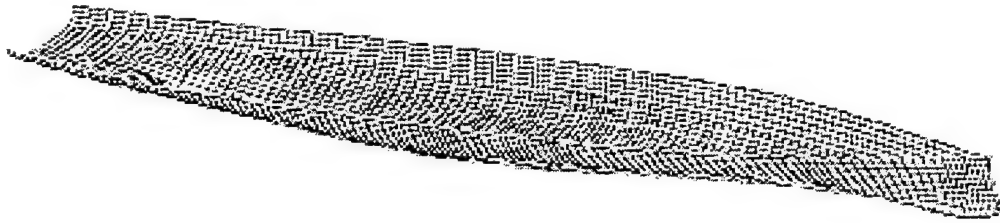

Figure D4: Single Element Liner (port side)
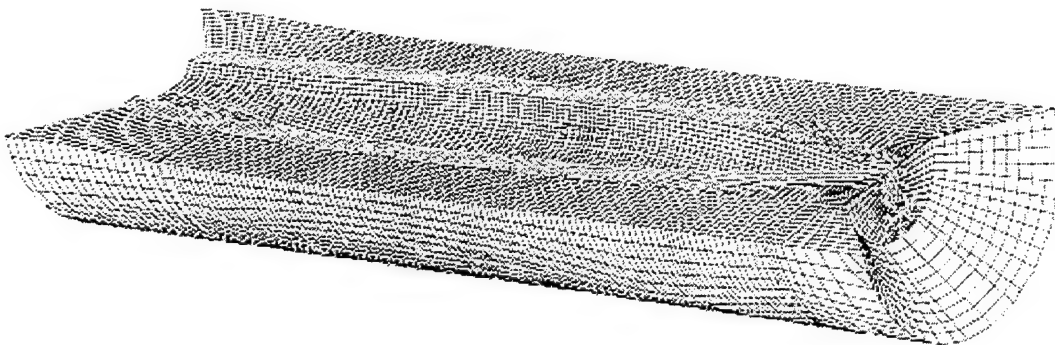
Figure D5: Complete Single Element Liner

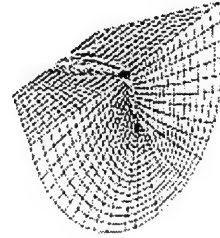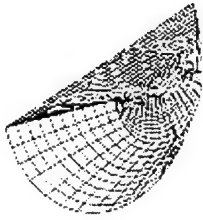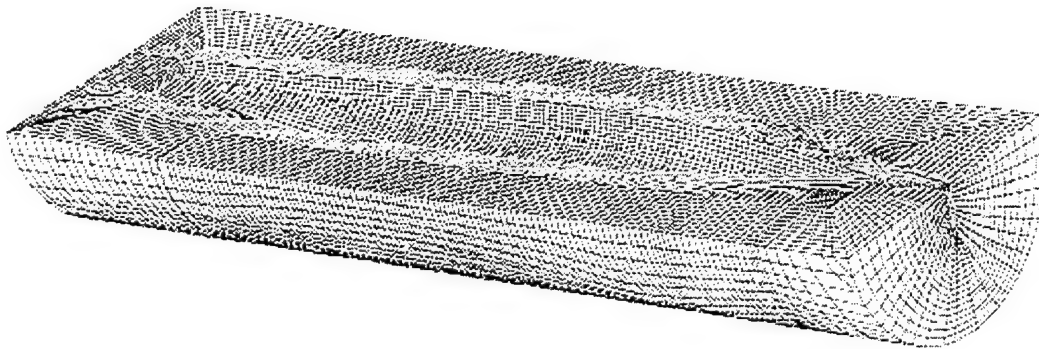**Figure D6: Inner and Outer Cylinder Mesh**

Figure D7: End Caps
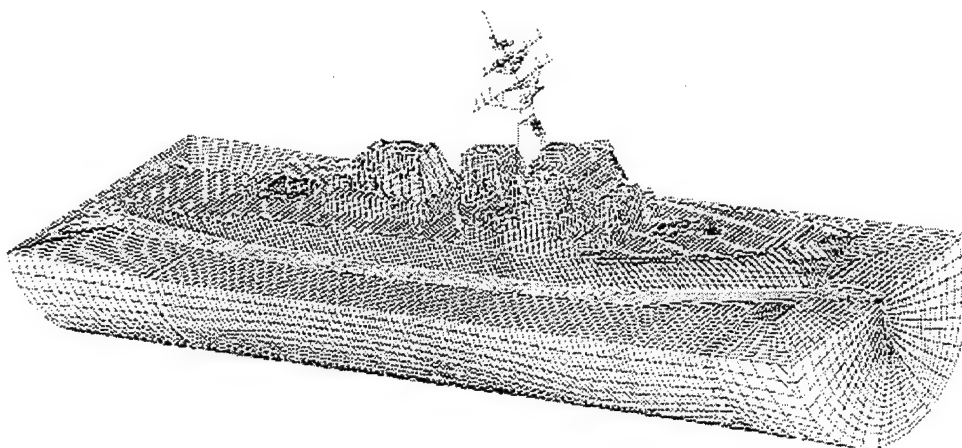
Figure D8: Completed Fluid Volume
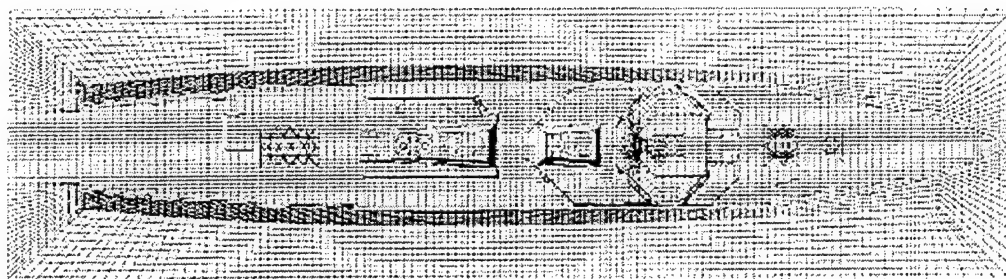
Figure D9: Coupled Ship and Fluid

Figure D10: Top View of Coupled Model

84

APPENDIX E: DAA1 ON WET SURFACE/NO FLUID VOLUME

For completeness a comparison is provided of the response of the barge model with and without the coupled fluid volume. Figure E1 shows the vertical velocity response of node 159 for the coupled and uncoupled cases. As can be seen in figure E2, the initial response at this node to the incident shock wave is similar. Both rise rapidly to approximately 25 ft/sec although the uncoupled model lags the coupled model slightly. The response curves then separate with the uncoupled model quickly dropping off to a constant positive velocity of approximately 2 ft/sec at 5-msec. The effects of cavitation are seen in the coupled model response as a higher peak velocity, longer decay time and larger amplitude rider frequency.

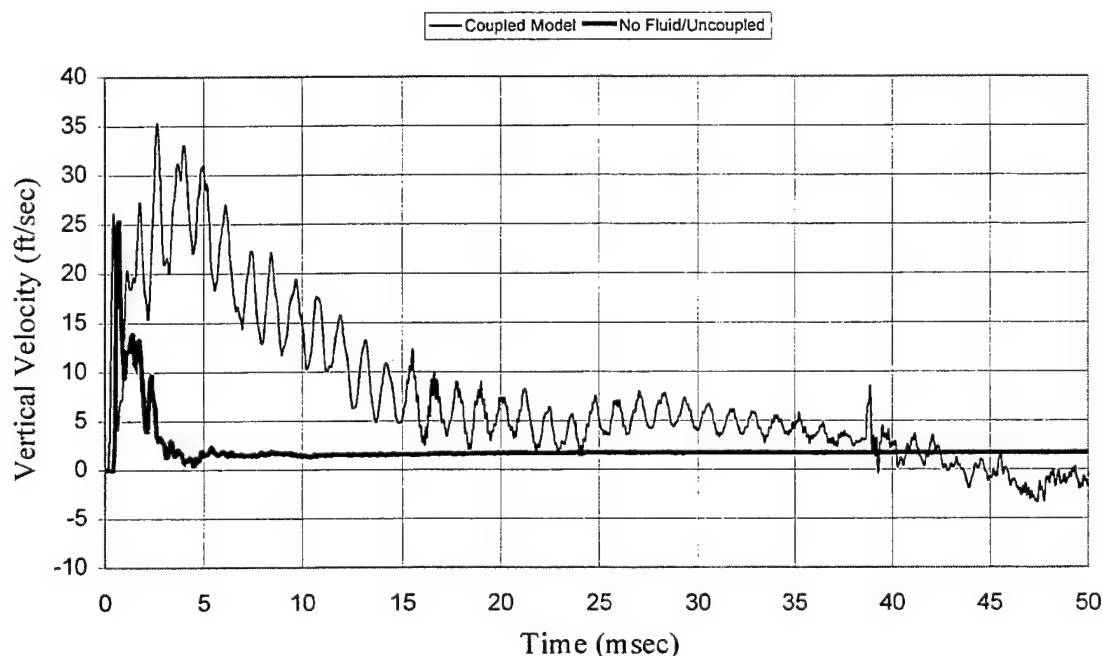### Coupled vs. Uncoupled Response for Node 159

Figure E1: coupled vs. Uncoupled Response for Node 159

85

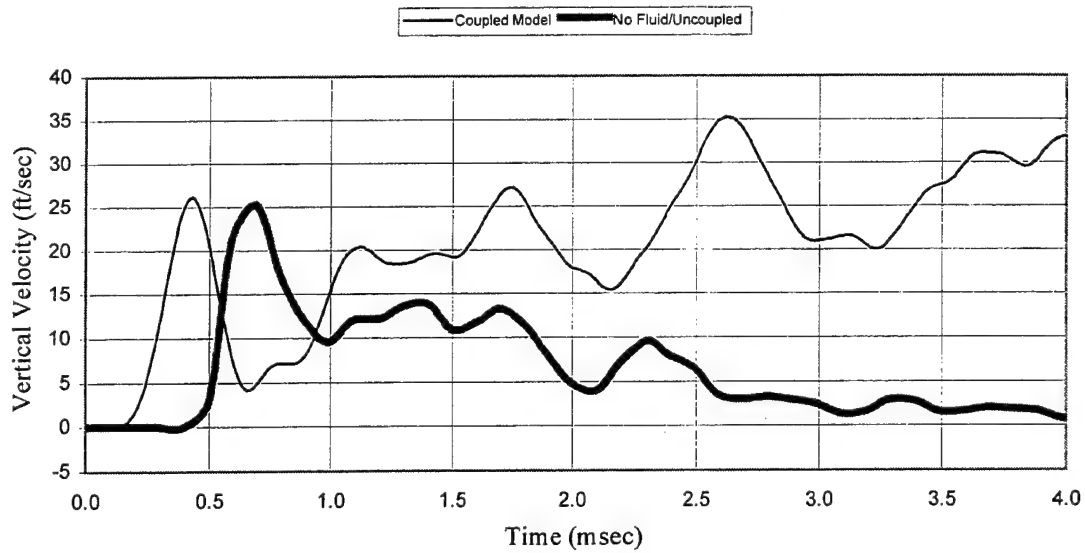**Coupled vs. Uncoupled Response for Node 159**

Figure E2: Initial 4-msec of Response of Node 159

Figure E3 shows the comparison of the models at node 213. This is the midships, centerline node. The response is damped at this location due to the flexibility of the plate and the presence of a lumped nodal mass.
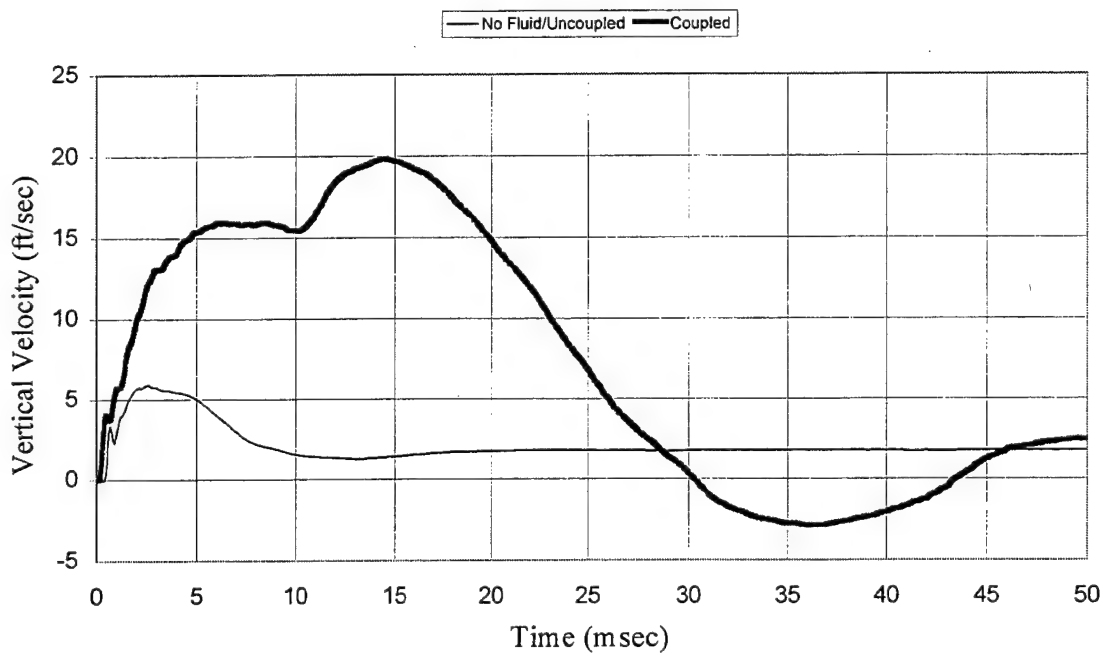
Coupled vs. Uncoupled Response for Node 213

Figure E3: Coupled vs. Uncoupled Response of Node 213

86

LIST OF REFERENCES

1. Underwater Explosions Research Division, "Fifty Years of RDT&E Experience", [www.dt.navy.mil/sites/uerd/history]. July 2000.

2. NAVSEA 0908-LP-000-3010A, *Shock Design Criteria for Surface Ships,* October 1994.

3. Military Specification, MIL-S-901D, *Shock Tests, High Impact Shipboard Machinery, Equipment and Systems, Requirements for*, March 1989.

4. OPNAV Instruction 9072.2, *Shock Hardening of Surface Ships*, January 1987

5. Mair, Hans U., Reese, Ronald, M., and Hartsough, Kurt, "Simulated Ship Shock Tests/Trials?", [www.dote.osd.mil/lfte/SSS.HTM]. July 2000.

6. USS John Paul Jones (DDG-53) Shock Trial Final Report, AEGIS Program Manager (PMS-400), November 1994.

7. Shin, Y.S. and Park, S.Y., "Ship Shock Trial Simulation of USS John Paul Jones (DDG53) Using LS_DYNA/USA: Three Dimensional Analysis", 70th Shock and Vibration Symposium Proceedings, Vol. I, November 1999.

8. XYZ Scientific Applications, Inc., *TrueGrid User Manual Version 2.0*, Livermore, CA, 1999.

9. Livermore Software Technology Corporation, *LS-DYNA Keyword User's Manual*, Version 950, Livermore, CA, 1999.

10. DeRuntz, J.A. Jr., "The Underwater Shock Analysis Code and Its Applications", Paper presented at the 60th Shock and Vibration Symposium, Vol. I, pp. 89-107, November 1989.

11. Cole, R.H., *Underwater Explosions*, pp. 3-13, Princeton University Press, 1948.

12. Shin, Y.S., "Naval Ship-Shock and Design Analysis", Course Notes for Underwater Shock Analysis, Naval Postgraduate School, Monterey, CA, 1996.

13. Wood, S.L., "Cavitation Effects on a Ship-Like Box Structure Subjected to an Underwater Explosion", Master's Thesis, Naval Postgraduate School, Monterey, CA, 1998.

14. Santiago, L.D., "Fluid-Interaction and Cavitation Effects on a Surface Ship Model Due to an Underwater Explosion", Master's Thesis, Naval Postgraduate School, Monterey, CA, 1996.

15. DeRuntz, J.A. Jr. and Rankin, C.C., "Applications of the USA-STAGS-CFA Code to Nonlinear Fluid-Structure Interaction Problems in Underwater Shock of Submerged Structures", 60th Shock and Vibration Symposium Proceedings, Vol. I, November 1989.

16. Bleich, H.H. and Sandler, I.S., "Dynamic Interaction Between Structures and Bilinear Fluids", International Journal of Solids and Structures, 1970.

17. Shin, Y.S., DeRuntz, J.A., "USA/LS-DYNA3D Software Training Course", Vol. V, July 1996.

18. Livermore Software Technology Corporation, *LS-POST User's Manual*, Version 1.0, Livermore, CA, May 1999.

19. Russel, D.D., "Error Measures for Comparing Transient Date: Part 2: The Error Measures Case Study",68th Shock and Vibration Symposium Proceedings, Vol. I, November 1999.

20. Geers, T.L., "An objective Error Measure for the Comparison of Calculated and Measured Transient Response Histories", The Shock and Vibration Bulletin, SAVIAC, NRL, Washington, DC, June, 1984.

21. Geers, T.L., "Validation of Computer Codes", Course Notes 1999.

22. Gibbs and Cox, Inc., "DDG53 Full Ship Finite Element Documentation (Draft)", Gibbs and Cox, Inc., May 1998.

INITIAL DISTRIBUTION LIST

1. Defense Technical Information Center..2
   8725 John J. Kingman Rd., Ste 0944
   Ft. Belvoir, VA 22060-6218

2. Dudley Knox Library...2
   Naval Postgraduate School
   411 Dyer Rd.
   Monterey, CA 93943-5101

3. Professor Young S. Shin, Code ME..4
   Department of Mechanical Engineering
   Naval Postgraduate School
   Monterey, CA 93943

4. Naval/Mechanical Engineering Curricular Office (Code 34)............................1
   Department of Mechanical Engineering
   Naval Postgraduate School
   Monterey, CA 93943

5. LT Philip E Malone 1
   1214 Lansing Ave W
   Bremerton, WA 98312

6. Michael C. Winnette...1
   Carderock Division
   Naval Surface Warfare Center
   9500 MacArthur Blvd.
   West Bethesda, MD 20817-5700

7. Gust Constant...1
   PMS400D5
   Naval Sea Systems Command
   2531 Jefferson Davis Highway
   Arlington, VA 22242-5165

8. Robert Rainsberger 1
   XYZ Scientific Applications
   1324 Concannon Blvd
   Livermore, CA 94550